INFORMATION TO USERS

This dissertation was produced from a microfilm copy of the original document. While the most advanced technological means to photograph and reproduce this document have been used, the quality is heavily dependent upon the quality of the original submitted.

The following explanation of techniques is provided to help you understand markings or patterns which may appear on this reproduction.

1. The sign or "target" for pages apparently lacking from the document photographed is "Missing Page(s)". If it was possible to obtain the missing page(s) or section, they are spliced into the film along with adjacent pages. This may have necessitated cutting thru an image and duplicating adjacent pages to insure you complete continuity.

2. When an image on the film is obliterated with a large round black mark, it is an indication that the photographer suspected that the copy may have moved during exposure and thus cause a blurred image. You will find a good image of the page in the adjacent frame.

3. When a map, drawing or chart, etc., was part of the material being photographed the photographer followed a definite method in "sectioning" the material. It is customary to begin photoing at the upper left hand corner of a large sheet and to continue photoing from left to right in equal sections with a small overlap. If necessary, sectioning is continued again — beginning below the first row and continuing on until complete.

4. The majority of users indicate that the textual content is of greatest value, however, a somewhat higher quality reproduction could be made from "photographs" if essential to the understanding of the dissertation. Silver prints of "photographs" may be ordered at additional charge by writing the Order Department, giving the catalog number, title, author and specific pages you wish reproduced.

University Microfilms

300 North Zeeb Road
Ann Arbor, Michigan 48106

A Xerox Education Company

THEORETICAL AND EXPERIMENTAL INVESTIGATIONS

OF THE

STRUCTURE AND PROPERTIES OF POLY-(trans-1,4-BUTADIENE)

by

JEANNE M. STELLMAN

A dissertation submitted to the Graduate Faculty in Chemistry in partial fulfillment of the requirements for the degree of Doctor of Philosophy, The City University of New York.

1972

This manuscript has been read and accepted for the Graduate Faculty in Chemistry in satisfaction of the dissertation requirement for the degree of Doctor of Philosophy.

May 9, 1972
date

Arthur E. Woodward
Chairman of the Examining Committee

May 9, 1972
date

Leonard H. Schwartz
Executive Officer

Professor A.E. Woodward

Professor D.J. Williams

Professor N. Yang

Supervisory Committee

The City University of New York

ACKNOWLEDGEMENTS

I wish to thank Professor Arthur E. Woodward for the support and guidance he has given me throughout the course of both my undergraduate and graduate education. In addition to extending to me his scientific skills, he and his family have always given to my husband and myself friendship and hospitality, which has always been very much appreciated.

I would like to acknowledge Professor Darrell Morrow of Rutgers University who opened his laboratory to me for the use of equipment without which this work could not have been done, and who also helped me with many enlightening discussions.

I also wish to acknowledge the appropriate granting agencies for the following fellowships: an NDEA Title IV Fellowship, a NASA Traineeship and a New York State Fellowship for Advanced Graduate Study.

Finally, I wish to thank my husband, Dr. Steven D. Stellman, who has always been at my side when I needed him. His excellent scientific skills and experience were of tremendous aid, especially in the theoretical section of this work. He has always put my needs first and tolerated with kindness the many anxious times I have provided him over the years.

TABLE OF CONTENTS

TABLE OF CONTENTS (cont'd)

TABLES

FIGURES

FIGURES (cont'd)

FIGURES (cont'd)

PART I

INTRODUCTION

Many of the basic concepts of polymer science were radically changed when it was reported that polyethylene (PE) could be precipitated from dilute solution in the form of small lamellar single crystals.[1] Since this initial discovery, single crystals from many polymers have been grown and studied[2] in an attempt to elucidate their morphology and the mechanisms of crystallization. Polymer single crystals are generally platelets on the order of 100 Å thick and several microns on a side. X-ray and electron diffraction reveal that the polymer chains preferentially orient normal to the surface of the crystals, along the 100 Å direction. Since the chains are much longer than 100 Å, they must, therefore, traverse the thickness of the crystal several times, somehow folding back on themselves at the surface. The nature of this fold surface has been the subject of intensive study and controversy.

The experimental studies to be described herein, involve quantitative chemical assays of the fold surface of poly-trans-1,4-butadiene (PTBD) as well as thermodynamic studies of the crystals as a whole. The experiments, in combination with theoretical thermodynamic calculations, described in Part II, are part of an ongoing study of the fold surface and crystal structure of PTBD single crystals.

Fold Surface Models

Several contradictory models have been proposed for the surface of PE single crystals. Some workers claim that the

polymer chains are regularly re-entrant[3-6] or enter the crystal at adjacent sites, but with the chain lengths within the fold varying slightly about some mean value.[7] Others picture the surface as loose and loopy and quite amorphous with the surface rather like a switchboard.[11,12] Several recent studies by Peterlin, Roe, Bair, Keller and others[13-15] seem to favor models in which there is a distribution of fold sizes, ranging from very tight to very long. All these models are, of course, consistent with transmission electron microscopy of the crystals, which is a direct examination of the surface, but which is incapable of disclosing details on molecular conformations.

The variety of models and the confusion that prevails arises because the surface alone is not accessible to direct experimental investigation. Rather, the experiments done are generally physico-chemical investigations of the crystals as a whole. The analysis of such quantities as mechanical data, heat measurements and infra-red spectra for surface models is uncertain because it is difficult to differentiate effects due to surface amorphousness or irregularity from defects in the interior of the crystals.

Krimm and co-workers[16,17] have been carrying out infra-red spectroscopy studies and theoretical analyses of the spectra of various deuterated PE crystals and have shown them to be consistent with a model of re-entrant folds on the surface. Koenig and co-workers[18,19] have been subjecting various polymer crystals to different physical conditions and then searching the infra-red spectra for changes in absorbance bands which correspond to changes

in the surface morphology. If a band is found to change in a consistent manner with the physical treatment, it is identified as a band due to regular folding on the crystal surface. To date, however, none of these studies have led to a quantitative determination of the length of the surface folds.

Attempts have been made to study the surface directly by chemical assay but the degradative chemical reactions employed have resulted in destruction of the crystals themselves, and again, the results are difficult to interpret. The reagent generally used for such studies has been fuming nitric acid.[8-10,20] In these investigations PE crystals were exposed to fuming nitric acid and the rates and extent of reaction followed. It was found that there was first a rapid reaction rate, followed by a markedly decreased rate. These kinetics were attributed to attack first of an easily accessible amorphous surface, followed by penetration into the crystalline interior, where because of steric hindrance, the reaction rate diminished. The extent of degradation seemed to indicate that the crystals were more than 50% amorphous, and that this amorphousness was almost all located in a very loose and loopy surface. Current work by Keller Priest and others[14,24] now indicates that the model is incorrect. Further study of the method indicates that the diminished rate is actually due to accumulation of degradation products blocking the reaction sites. Apparently there is no reaction rate difference between amorphous and crystalline PE with a reagent as powerful as fuming nitric acid. They conclude that milder degradative techniques are necessary.

In another series of studies, degradation products from

nitric acid reacted PE crystals were analyzed by gel permeation chromatography[20-22] (GPC) for molecular weight distributions. It was found that two peaks in a 2:1 ratio dominated the chromatogram. They were attributed to molecular weight fractions corresponding to single chain and double chain traverse lengths that were scissioned by nitric acid. This work has also been re-interpreted[14] as indicating that the surface consists of chains of various lengths, buried at different depths in the crystals. As the chains are cut at various locations, more are exposed, and the cut chains are constantly being degraded. Thus the peaks corresponding to longer chains diminish and shift to lower molecular weight regions. This result has also been found in annealed PE single crystals.[23]

Another oxidation technique, treatment with ozone gas, has been used on PE crystals.[25-27] Here too the reaction was followed by GPC as well as by the increase in weight and density, quantitative chemical reaction of carboxyl groups with dilute NaOH, and infrared spectroscopy of functional groups. The same shifts in GPC peaks were observed, and the kinetics were consistent with those found upon fuming nitric acid treatment. These experiments have been interpreted[14] as confirming the model of adjacently reentrant folds of various lengths, terminating at different depths within the crystal.

Another feature of the surface of the crystals is the presence of non-reentrant chain ends or cilia. Estimates have been made that if the length of the chain end is less than a single traverse of the lamella, the chain will remain on the surface as a non-reentrant end.[26] Infrared studies of these chain ends[28] and

chemical reaction with subsequent thermal treatment, also lead to this conclusion.[27]

Based on the preceding discussion, it is clear that the exact nature of the surface folds is still undiscovered. Moreover, the need for a nondegradative quantitative method of assaying the surface morphology of polymer single crystals is apparent. For this reason, poly-trans-1,4-butadiene (PTBD), an unsaturated polymer, was selected for use in this study. The double bond in the repeat unit reacts quantitatively with many reactants; and,

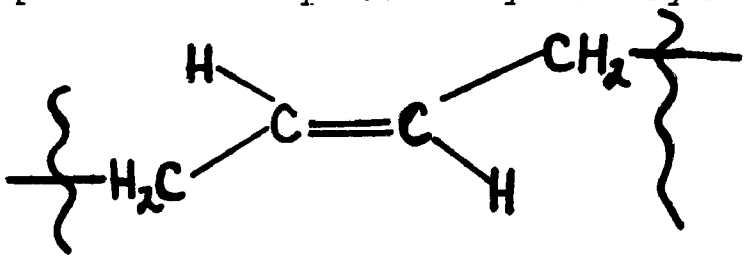

PTBD

specifically, the peroxidation of the double bond in polybutadiene is an extremely accurate and sensitive quantitative technique.[29,30] It can be used to disclose the number of double bonds that are available for reaction , and thus the double bond in PTBD serves as a "chemical handle" on the surface folding phenomenon. Moreover, with this technique which doesn't damage the crystals in the course of reacting, it is possible to assay the effects of different growth conditions, solvents and molecular weights on the number of double bonds available. In combination with accurate data on the crystal structure of PTBD[31,32] and thickness measurements, knowledge of the number of bonds available for reaction can lead to a good estimate of the tightness of folds on the surface of various PTBD single crystal preparations. In combination with this, crystals grown from lower molecular weight polymer would

have a different percentage of polymer present as non-reentrant chains if previously discussed models are valid. Such differences would be revealed in the chemical reaction of surface double bonds as well.

Single crystals of PTBD can be readily grown from a variety of solvents.[33] A minimum dissolution temperature growth method was developed that readily produced preparations of regularly shaped, uniform crystals. Hence, PTBD is most suitable for a study of the fold-surface character of single crystals.

Thermal Properties and Crystal Structure

Since polymer single crystals are expected to have interfacial irregularities as well as internal defects, they should exhibit deviation from the thermodynamic behavior expected of perfectly crystalline materials. Numerous papers have been published on the thermodynamic properties of PE single crystals and have led to various estimates for the surface free energy and entropy.[13,34] These estimates, in turn, have been used to approximate the number of segments in the fold surfaces. Roe and Bair[13] have calculated that the average number of $-CH_2-$ segments in the PE single crystals fold is about 20, with some of the folds very tight and others much larger than 20 segments long.

Other studies have been made to determine the relationships between crystallite thickness, equilibrium dissolution temperature, and the various measureable thermodynamic quantities.[35,36] It is generally agreed that the crystallite thickness, ρ, is dependent on crystallization temperature[34,35,37-39] and indepen-

dent of storage time at the crystallization temperature, as well as independent of molecular weight.[40] This is in contrast to bulk crystallized samples which are found to have thermodynamic properties very dependent on molecular weight.[41,42] By detailed comparison of the mechanical and thermodynamic properties, the infrared spectra, x-ray diffraction and density measurements of bulk samples and single crystals, Mandelkern and co-workers have concluded that the differences in behavior can be attributed solely to an amorphous surface layer on the single crystals.[43]

Finally, very general considerations led Mandelkern, Sharma and others[35,44] to equate the measured enthalpy of fusion, per repeat unit, ΔH^*, to the degree of crystallinity, $1-\lambda$, of the crystals:

$$\frac{\Delta H^*}{1-\lambda} = \Delta H_u - \frac{2\Delta H_e}{\mathcal{L}} + \alpha \Delta H_d \qquad (1)$$

where ΔH_u is the theoretical enthalpy of fusion per repeat unit for perfect crystals, ΔH_e is the enthalpy deficiency per sequence at the surface of the crystals, $\mathcal{L}$ is the crystallite thickness, α the fraction of defective units per sequence in the interior of the crystal, and ΔH_d is the enthalpic contribution from interior defects.

Thermodynamic studies can be useful in elucidating structural properties of materials. No such studies have been reported for PTBD single crystals, although thermal data on bulk crystallized PTBD are available.[26,27] Thus the thermal proper-

ties of PTBD single crystals and how they can be related to the crystal structure would be of interest. In addition, PTBD undergoes a reversible first-order solid-solid phase transition, for which bulk studies show the entropy of transition to be almost twice the entropy of melting. This makes calorimetric investigations of PTBD an even more interesting undertaking.

PTBD single crystals grown from various solvents show different dynamical-mechanical behavior,[33,47] as well as differences in the infra-red spectra.[48] Tatsumi et al. have attributed the larger dynamical relaxations of benzene-grown PTBD crystals to a loose and loopy surface. The infra-red spectra were found by Hendrix, Whiting and Woodward, to have a regularity band (1335 cm^{-1}) and an amorphous band (1350 cm^{-1}) whose ratio varied with the solvent used for the preparation as well as with the thermal history of the sample. Since calorimetry is a good analytical method for determining crystallinity of polymer samples, it was felt that differential scanning calorimetry might provide further insight into differences in surface and internal structure of crystals grown from various solvents or subjected to thermal treatment.

The crystal structure of the low-temperature form of PTBD has been reported.[31] Data on the lattice packing of the high temperature form is also available[32] although completely unambiguous crystallographic data has not been obtained as yet. Since the solid-solid phase transition takes place between two forms of known geometries, theoretical calculations of the energies of transition can be made without resorting to the typical approxi-

mations made in such calculations (such as representing the energy of the polymer in the melt with a single chain[47-52]). These calculations will be discussed in detail in Part II. However, in order to maximize the amount of information obtainable from theoretical considerations, it is necessary to obtain accurate thermal measurements of the heat of the phase transition, as well as accurate heat capacity measurements of PTBD, for comparison with theoretically derived values.

Thus the experimental work to be described in Part I involved both quantitative chemical assay of the surface of PTBD single crystals and calorimetric studies of PTBD, and are part of an attempt at providing more definitive understanding of the structure of PTBD single crystals.

EXPERIMENTAL

Samples

Samples of PTBD were obtained from two sources. The majority of experimental work was done on PTBD obtained by Prof. M. Takayanagi from Ube-Kosan Co., Ltd., of Japan (PTBD-K). It was found from infrared analysis, using a Perkin-Elmer 621 Spectroscope and routine scanning conditions, that the trans content of this sample was greater than 95%. The number average molecular weight, $\overline{M_n}$, of the sample as received was found to be 8670 (± 10%), which leads to a number average degree of polymerization, $\overline{DP_n}$, of 160. For a sample of PTBD-K crystals recovered from n-heptane solution, as described below, $\overline{M_n}$ was found to be 36,900 (± 10%). The $\overline{M_n}$ was obtained by DeBell and Richardson Co., Inc., using a Hitachi-Perkin-Elmer vapor phase osmometer. A second sample of the polymer, PTBD-U, was obtained from Dr. Robert Rinehart of Uniroyal, Inc. Infrared examination of this sample showed it also to be greater than 95% trans.

Viscosity-average molecular weights, $\overline{M_v}$, were determined for both samples, using the following relationship derived by Endo[53] for PTBD:

$$[\eta] = 2.9 \times 10^{-4} \overline{M_v}^{0.75} \qquad (2)$$

where $[\eta]$ is the intrinsic viscosity. The intrinsic viscosities were determined with a Ubbelhode dilution viscometer, at 30° C., using chloroform as a solvent. The intrinsic viscosities and the $\overline{M_v}$ were:

PTBD-K	$[\eta] = 1.53$ dl/g	$\overline{M_v} = 92{,}000$
PTBD-U	$[\eta] = 0.32$ dl/g	$\overline{M_v} = 11{,}000$

Growth Techniques

Single crystals of PTBD can be readily grown and a growth technique was developed which produced well-formed uniform crystal preparations from several different solvents. The dissolution temperature used for the bulk sample affected the morphology of the crystals. When the minimum dissolution temperature was employed, very regular crystal preparations were obtained from n-heptane, methyl isobutyl ketone (MIBK), and toluene solutions. This technique is similar to that concurrently developed by Blundell and Keller[54] for PE single crystals. In their method for producing uniform growths, the redissolution temperature of the sample was critical.

The following procedure was used to obtain the crystals. Bulk polymer and solvent were added to a 25 ml test tube to give 0.02% solutions. The tubes were then placed in a constant temperature water bath at the minimum temperature needed for dissolution. After the samples were dissolved, the solutions were filtered throught a coarse sintered glass filter, using a water aspirator, and then allowed to precipitate quickly at room temperature. Whenever toluene was the solvent, rapid pre-precipitation was achieved by placing the tube in an ice bath. Examination of these precipitates under an optical microscope showed them to be rough, over-

grown, and irregular. The pre-precipitates were then redissolved at the original dissolution temperature and immediately placed in a thermostated oil bath, regulated to ±0.1°C., until precipitation was complete. This technique, however, did not produce crystals of PTBD-K when benzene was used as a solvent. Crystals were grown from benzene using the technique of Hendrix et al.[48] which simply involved dissolution at 52°C (not the minimum dissolution temperature), filtration, and isothermal growth at 8°C. The growth conditions are summarized in Table I.

TABLE I. Growth conditions for PTBD Single Crystals.

Sample	Solvent	Dissolution Temperature	Growth Temperature	%ppt
PTBD-K	MIBK	92°C.	73°C.	——
	heptane	76	63	75
	toluene	50	23	40
	benzene	52	8	35
PTBD-U	heptane	69	50	25

Another effect of the dissolution temperature on PTBD single crystals was noted in that the lateral-side dimensions of PTBD-K crystals grown from heptane or MIBK were a function of dissolution temperature.

Figures 1 through 4 show representative fields of crystals grown and studied. The electron micrographs were taken on a Phillips 300 electron microscope. Selected area diffraction patterns of the various types of crystals were also taken. One preparation, PTBD-K crystals grown from n-heptane, was fil-

tered into a mat and the solvent was removed using a water aspirator. This mat was then placed in a Debye-Scherrer powder camera in such a way that the beam would penetrate the thickness of the mat. The crystals were exposed to Cu Kα radiation at 15 ma and 10 kv for one hour, and a fiber pattern film was developed.

Chemical Assay Technique

The quantitative epoxidation reactions of the available double bonds were performed in the following manner. Previous studies[29,30] with perbenzoic acid and rubbers consisting of a mixture of polybutadienes had shown that the reaction is an extremely sensitive quantitative technique that can even be used to differentiate among the various geometric isomers and the 1,2 and 1,4 linkages in butadiene. Perbenzoic acid, however, is quite unstable and decomposes rapidly. For the extended lengths of time necessary for complete reaction with the single crystals, the decomposition rate of the acid was as great or greater than the rate of the reaction itself. Therefore, the procedure was modified and meta-chloroperbenzoic acid (m-ClØCOOOH) was used as the peroxidizing agent in the following reaction:

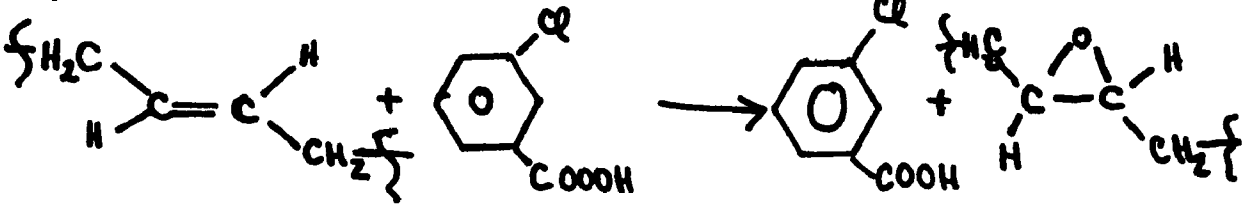

The presence of the electronegative chlorine group in the meta position serves to stabilize the peracid group on the ring so that decomposition is significantly decreased.

Sufficient tubes of PTBD were grown to give between 0.06 and 0.09 g of single crystals. The crystals were separated from the mother liquor by hot filtration and washed with fresh, hot solvent. The crystals always remained in suspension and were not allowed to dry out or mat together. The mixture was then resuspended in cold benzene, m-ClØCOOOH added, and the reaction mixture placed in a refrigerator at 0°C. The amount of polymer present was determined in two ways. For n-heptane grown crystals the amount of polymer left in the mother liquor was found and the weight of polymer was determined by difference. For the other preparations, the samples were made into mats and weighed after the reaction was complete. The amount of polymer and acid used varied in the different reaction mixtures; these quantities are shown in Table II.

A control solution of the same concentration of m-ClØCOOOH was also refrigerated under the same conditions as the reaction mixture to ascertain the effectiveness of the peracid, as well as to follow its decomposition, if any, during the course of the reaction. The extent of peroxidation was determined by standard iodometric titration of the peroxyacid remaining. Aliquots of 0.5 ml were removed at various intervals. The reaction was followed for at least 48 hours after

TABLE II. Relative Composition of Peroxidation Reaction Mixtures.

Sample	Solvent	Reaction #	Ratio (-OOH/double bonds)
PTBD-K	Heptane	7	20%
		9	42%
		12	18%
PTBD-K	MIBK	1	26%
		2	41%
		3	26%
		4	23%
PTBD-K	Toluene	1	26%
		2	23%
PTBD-U	Heptane	1	135%

no further disappearance of acid was noted. Enough crystals were also removed after each time interval for examination under the electron microscope for both selected area diffraction and transmission micrographs.

A benzene solution of bulk PTBD was also reacted with m-ClØCOOOH at 18°C. to test whether the reaction would go to completion if all double bonds were available for epoxidation.

Representative crystals of each type were shadowed with Pt-Pd or Au-Pd and preliminary thickness measurements were made by measurement of the shadpw lengths. More accurate thickness measurements were carried out by Dr. Brian Newman, at Rutgers University, using a Rigaku-Denki small-angle goniometer X-ray apparatus. The low angle scans were made on filtered single crystal mats that remained under suction until the solvent was removed.

Differential Scanning Calorimetry

Differential scanning calorimetry (DSC) studies were also made of PTBD single crystals grown from various solvents. The scans were run on a Perkin-Elmer DSC-1B scanning calorimeter and the specific heat measurements of heptane-grown crystals and melt-recrystallized sample carried out with the specific heat kit attachment for the DSC-1B. All scans were made using the maximum sensitivity that kept the peak on the recorder paper, and at the fastest chart speed, in order to maximize the size of the peak. The scan rate was generally

20°C. per minute, but several runs were made at much slower rates to ascertain whether thermal rearrangements were occurring. All scans were made using the routine procedures described in the Operating Manual.

Heptane crystal mats and toluene crystal mats were sealed in evacuated glass ampules and subjected to electron beam irradiation, in order to lightly cross-link the surface. The toluene crystals were irradiated for three minutes and the heptane for six minutes at 1. MeV and 0.44 $\mu A/cm^2$. Thermographs of these samples were taken as a second test for possible thermal rearrangement of the crystals.

All samples were weighed on a Cahn electrobalance and several different experiments were performed. Some samples were simply taken through the transition, melted, recrystallized, and taken through the transition again. Other samples were taken through the transition, annealed for a length of time that varied between 30-63 minutes, at a temperature a few degrees above the transition, and then subjected to further thermal study, of the kind described above. Representative thermograms appear in Figs. 10-12.

The heat of fusion, ΔH_f, and the heat of transition, ΔH_{tr}, were determined in the following manner. The area under the transition curve was measured using a Keuffel and Esser compensating polar planimeter. This procedure was more precise than cutting out and weighing the peaks. Two standards, indium and tin, whose ΔH_f are accurately known, were also melted on the DSC-1B, under the same operating conditions as

the PTBD samples. The area under the standard curves was measured and these areas were equated to the known ΔH_f. Thus a calibration of the number of calories per unit area was found.

Transition temperatures were all determined in the following way. The baseline was drawn in for each curve. The temperature of transition was read at the point where the curve first departs from the baseline. The temperature at which the transition is proceeding at the maximum rate is that which corresponds to the maximum height of the curve. The temperature scale was calibrated using tin and indium standards.

Unlike scanning calorimetry, specific heat measurement is much more dependent on several experimental parameters.[55] Whereas the standard calorimetric run requires a sample weight of only about 1 mg, at least 15 mg of crystals were necessary to achieve a reproducible result. The specific heat technique used is the standard one described in the Operating Manual. First a sapphire (aluminum oxide) standard, whose specific heat is accurately known for the entire temperature range studied, is run on the machine. The sapphire scan must return to within 4% deflection of its starting position. The sensitivity, slope, and scan speed are adjusted until this criterion is met. Then, in the same sample pan, with the cover aligned in the same direction for the same heat deflection, the empty sample pan is run to establish a baseline that is due to the machine alone. Finally, the sample is run, again in the same pan and in the same position. The sample was made up of

many single crystal mats which were piled on top of one another and punched into a circular shape with a standard hole punch. The uniformity of shape is important for uniform heat conduction. The mats were almost the exact diameter of the sample pan. Reproducible data on the single crystal mats was not obtained because of machine operating difficulties. The results presented are from scans of the melt-recrystallized heptane grown crystal mats.

The temperature range was broken up into several scans of about 30-40° each because there is too much baseline shift over a wider range. The machine was recalibrated for the sapphire and the baseline in each range. At the end of each temperature interval, the calorimeter is stopped and the pen allowed to re-establish a baseline at the upper temperature. For the calculations, the beginning and ending baselines were connected. It was not possible to re-establish a baseline after melting of the sample because of the extremely wide drift of the pen. Therefore, the heat capacity of the sample was measured only up to 110°C. The specific heat of the sample is calculated by comparison with the known specific heat of the sapphire, at each temperature. The deflection due to the baseline shift is subtracted from the sample and sapphire. Thus at each temperature, a deflection is equated to a known specific heat and the value for the crystals is then calculated.

RESULTS

Figures 1 through 4 are representative transmission electron micrographs of the PTBD single crystals grown from various solvents, by the minimum dissolution temperature technique. As can be seen, this growth technique produces crystals of uniform size. Figure 5 is a typical selected area diffraction pattern obtained from heptane crystals. The same patterns were obtained from all the crystals. These patterns and the X-ray pattern taken on the single crystal mat were all in agreement with previously published structural data.[31]

The percentage of polymer precipitated during the single crystal preparations from a solution of the bulk material is similar for PTBD-K from the three different solvents used, but is much lower for the PTBD-U - heptane system (Table I). The crystallization process for the PTBD-K leads to a fractionation of the bulk material, as is evident from the change in $\overline{M_n}$ reported in the previous section. The bulk PTBD-U is believed to be less polydisperse than the bulk PTBD-K, but it also has a lower $\overline{M_v}$, which may account for the fact that its minimum dissolution temperature in heptane is 9°C. lower than the PTBD-K. It may also account for its higher solubility in n-heptane at the precipitation temperature employed.

Many of the crystals obtained from the MIBK solution have holes and rough surfaces, as seen in Fig. 3. These interesting effects were incurred during the crystal preparation and/or isolation, and are not due to subsequent thermal

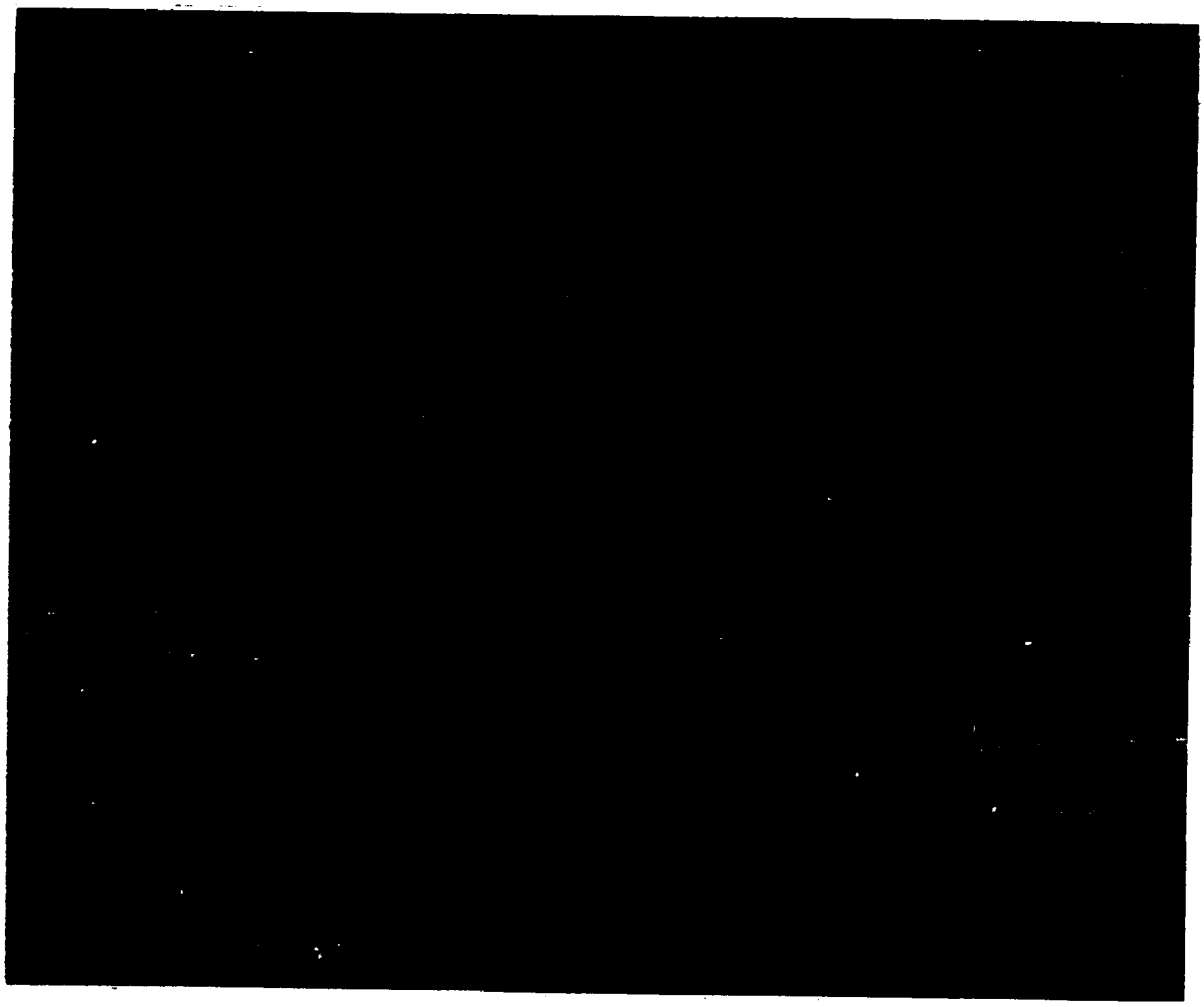

FIGURE 2. PTBD crystals grown from toluene.

FIGURE 4. PTBD-U crystals grown from n-heptane.

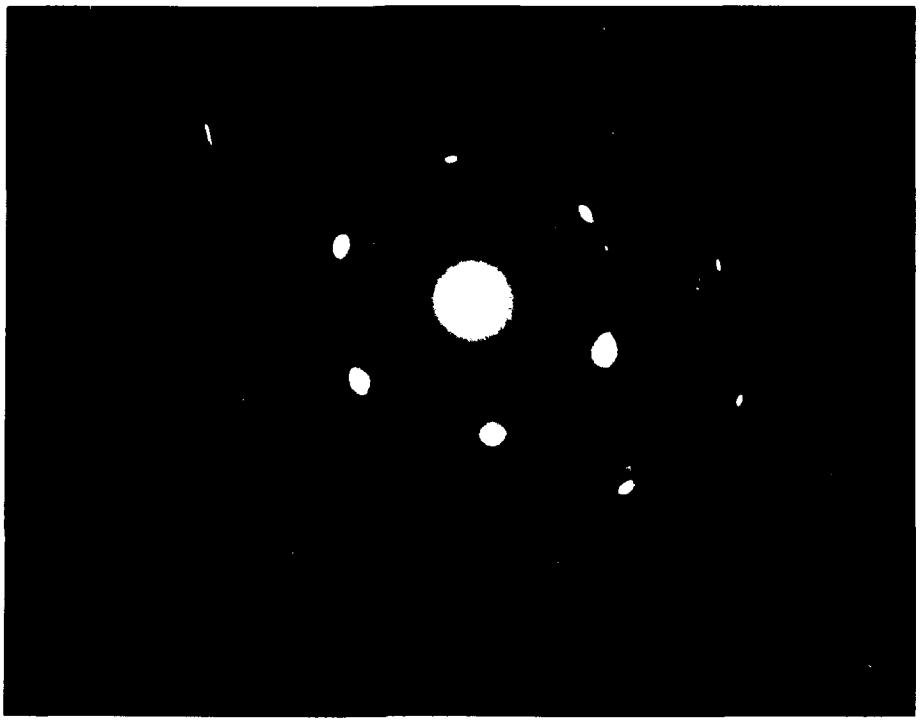

FIGURE 5. Selected area diffraction pattern for n-heptane grown PTBD crystals.

treatments (annealing) known to yield thicker hole-ridden crystals.[2] Other interesting size effects were observed; the PTBD-K crystals from toluene were consistently smaller by a factor of about 2 than those from n-heptane and MIBK. An increase in dissolution temperature in the 92-103°C. range for MIBK crystals grown at 73°C. resulted in an increase in crystal size. Average diameters of 3, 8, and 48μ were observed when dissolution temperatures of 92°, 97°, and 103°C., respectively, were used. For PTBD-K heptane crystals, a change in dissolution temperature from 78 to 88°C. resulted in a change of crystal diameter from 4 to 20μ, when the precipitation temperature was 63.5°C. The same effect was reported[54] previously for polyethylene crystals, although it was the temperature at which the precipitate was redissolved which was critical for this case.

Titration Results

Table III summarizes the results of the titration studies in terms of the number of runs and mean values of the percentage of double bonds available. Although there were differences in the rates of double bond disappearance at times below 100 hours for the toluene and heptane crystals, and 150 hours for the MIBK crystals, a leveling off of the percentage of double bonds reacted occurred at later times. The crystal thickness cited for the PTBD-K heptane and toluene preparations were determined by low angle X-ray. The value for heptane crystals is not in complete agreement with those previously

TABLE III

Determination of Available Double Bonds on PTBD Crystals

Sample	Solvent	(Minimum) dissolution temperature, °C	Precipitation temperature, °C	Precipitate, %	Crystal thickness Å	No. of epoxidation determinations	Double bonds reacted %	No. monomer units/fold	
								Uncorr.	Corr[a]
PTBD-K	Heptane	78	63.5	78	110±6	3	14	3.2	2.5
PTBD-K	MIBK	92	73	68	130±15	4	22	6	5
PTBD-K	Toluene	50	23	76	103±6	2	18	3.5-3.7	3
PTBD-U	Heptane	69	53	13	95±10	1	28	5.5	3.5

[a] Value corrected for double bonds in chain ends (see text)

reported[57] as estimated from shadow castings. This discrepancy is probably due to the fact that the edges of the single crystals from heptane curl considerably, leading to enlarged shadows. The PTBD-K-MIBK and PTBD-U-heptane crystal thicknesses were estimated from the shadow castings.

Figures 6 to 8 are plots of the percentage double bonds reacted for each solvent system. The data for the PTBD-U heptane were not plotted. Figure 9 shows all three systems plotted on the same graph. From transmission electron micrographs of crystals removed after the reactions had levelled off, all had an appearance similar to that of the unreacted crystals. Selected area patterns were also unchanged. When the PTBD solution was titrated to test for completeness of reaction with all double bonds accessible, 70% of the double bonds reacted within 5 minutes, and the reaction was complete after 24 hours. All of this evidence, coupled with the fact that the reactions levelled off, indicates that the reaction was restricted to the surface.

In one case, however, the titer of PTBD-U-heptane crystals began to rise after 100 hours. Subsequent electron microscopy by Hendrix et al.[48] indicated that the reagent may be penetrating the crystals in some runs for this particular preparation. The mean value reported in Table III is that found in the first 168 hours. Since titration values do not rise steadily, but fluctuate randomly around this mean value, the value was taken to be the correct one prior to penetration

Figure 6
Percentage of double bonds in MIBK-grown PTBD crystals reacted with meta-chloroperbenzoic acid versus time for four separate reaction mixtures.

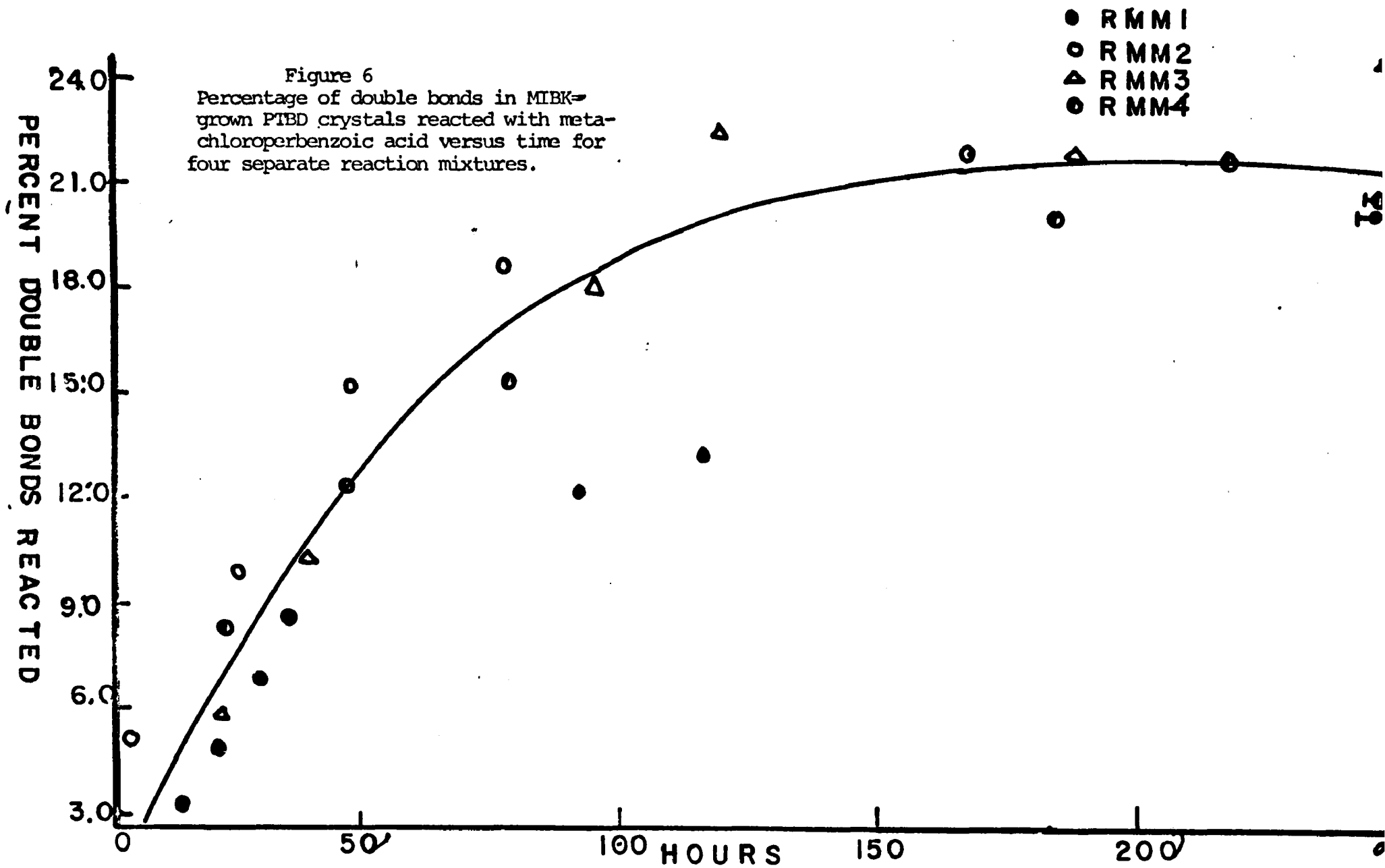

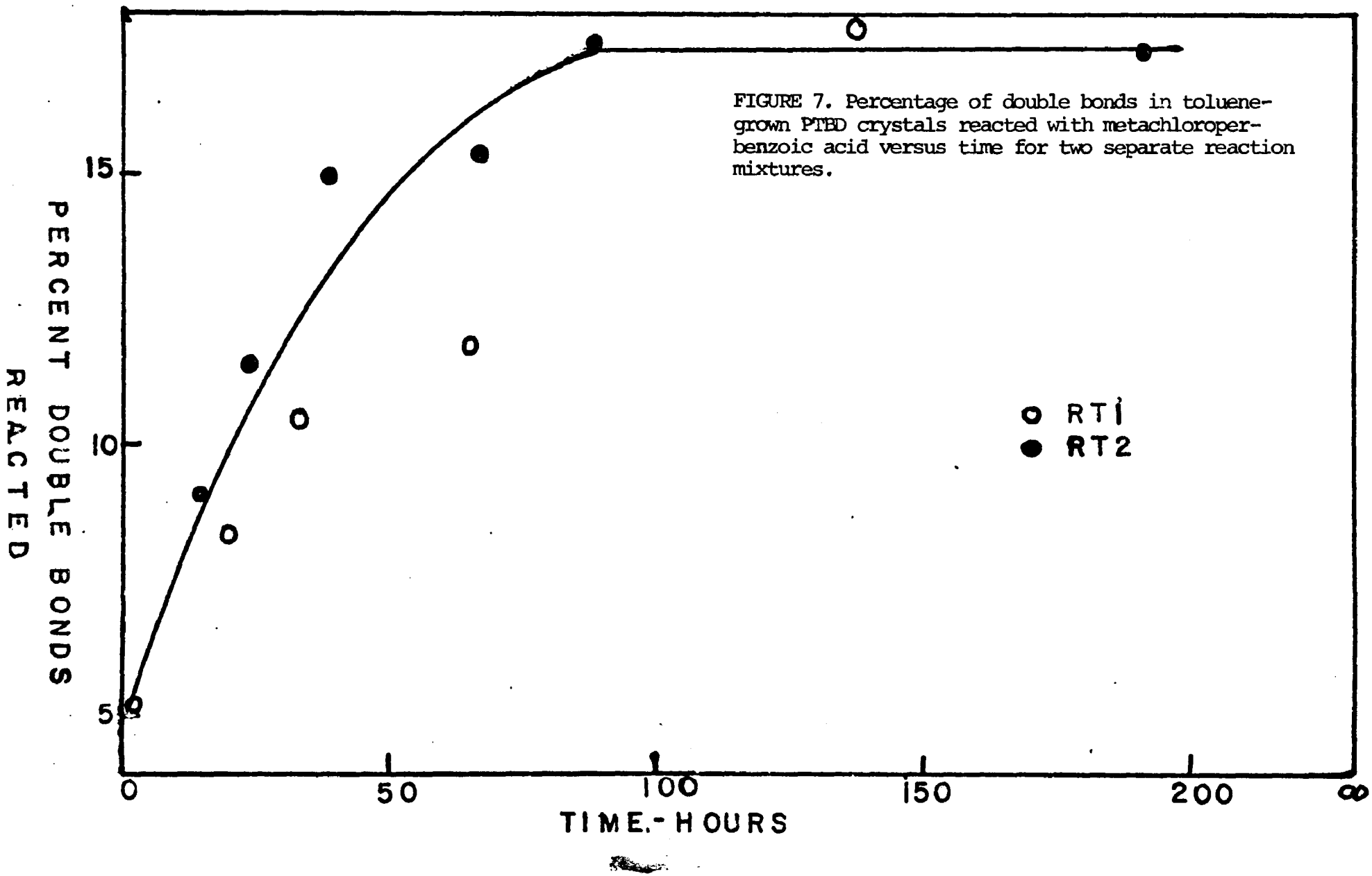

FIGURE 7. Percentage of double bonds in toluene-grown PTBD crystals reacted with metachloroperbenzoic acid versus time for two separate reaction mixtures.

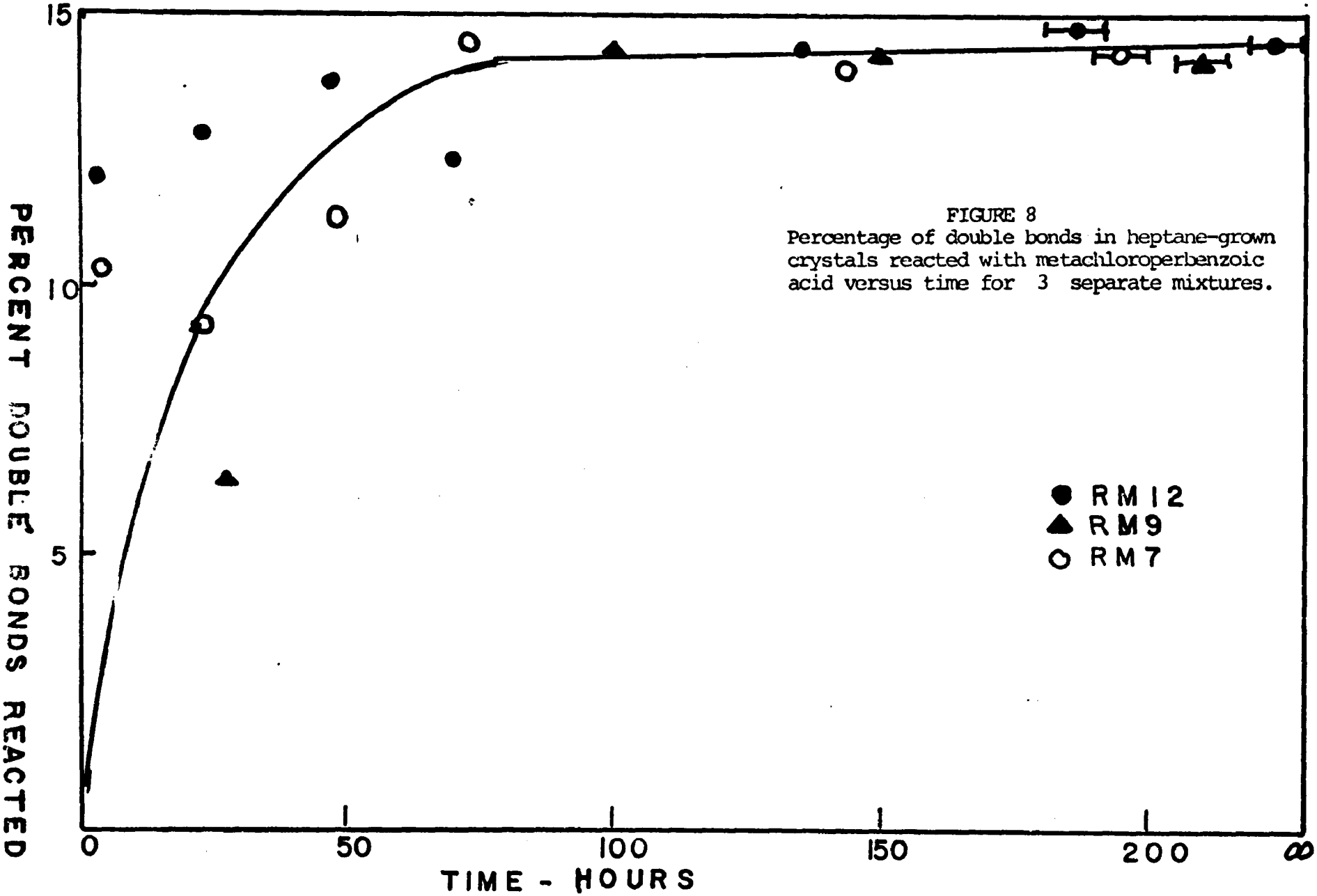

FIGURE 8
Percentage of double bonds in heptane-grown crystals reacted with metachloroperbenzoic acid versus time for 3 separate mixtures.

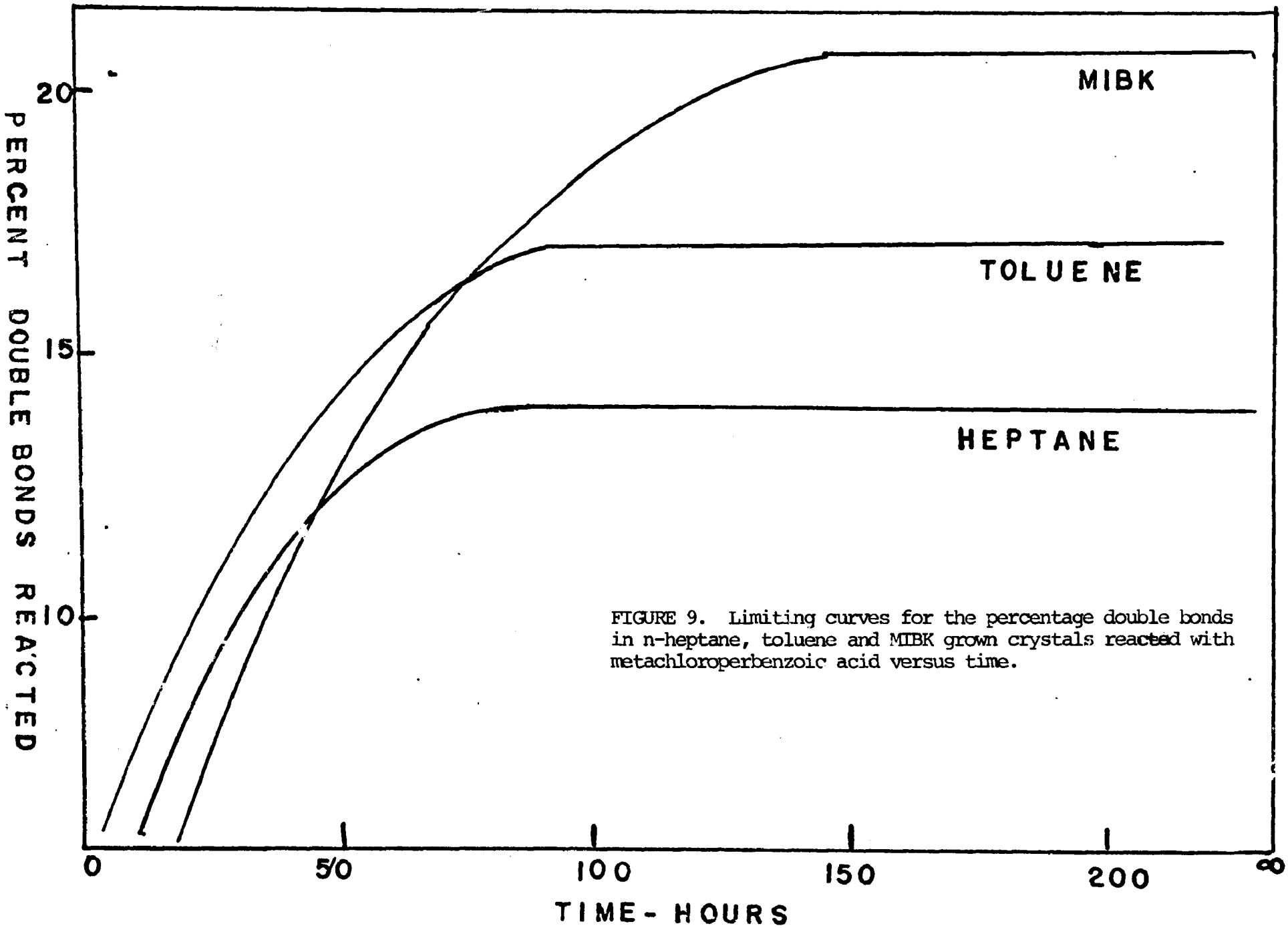

FIGURE 9

FIGURE 9. Limiting curves for the percentage double bonds in n-heptane, toluene and MIBK grown crystals reacted with metachloroperbenzoic acid versus time.

of solvent into the interior of the crystal. In addition, electron microscopy revealed no penetration.

Calorimetry Results

Figures 10 to 12 are typical scans of PTBD crystals grown from heptane, toluene and benzene. Table IV contains the measured heats of melting, recrystallization and transition. The heats of transition of the crystals annealed below the crystalline melting point were not tabulated because reproducible results were not obtained. The peaks for these transitions were erratic for all preparations in that some crystals never showed a transition after annealing, whereas others had peaks that were split into several smaller ones. For those runs with regular peaks, where planimetry was possible, no pattern emerged. Some of the heats were smaller than the original heat of transition, others were larger. This may be due to the fact that the samples were cooled down at the scan rate of 20°C/minute, which may not have allowed the crystals to re-equilibrate.

Unlike PE[39], PTBD crystals do not seem to undergo thermal rearrangements and lamellar thickening during the scans through the transition. The evidence for this is that the peaks obtained are regular and sharp, and similar in shape to the peaks obtained from the melt-recrystallized sample, whereas PE single crystals exhibit multiple peaks of irregular shape. Additionally, the first two values for the PTBD-benzene crystals listed in Table IV correspond to scan rates of 20°C/minute and 40°C/minute, respectively. If thermal rearrangements were occurring, one would expect

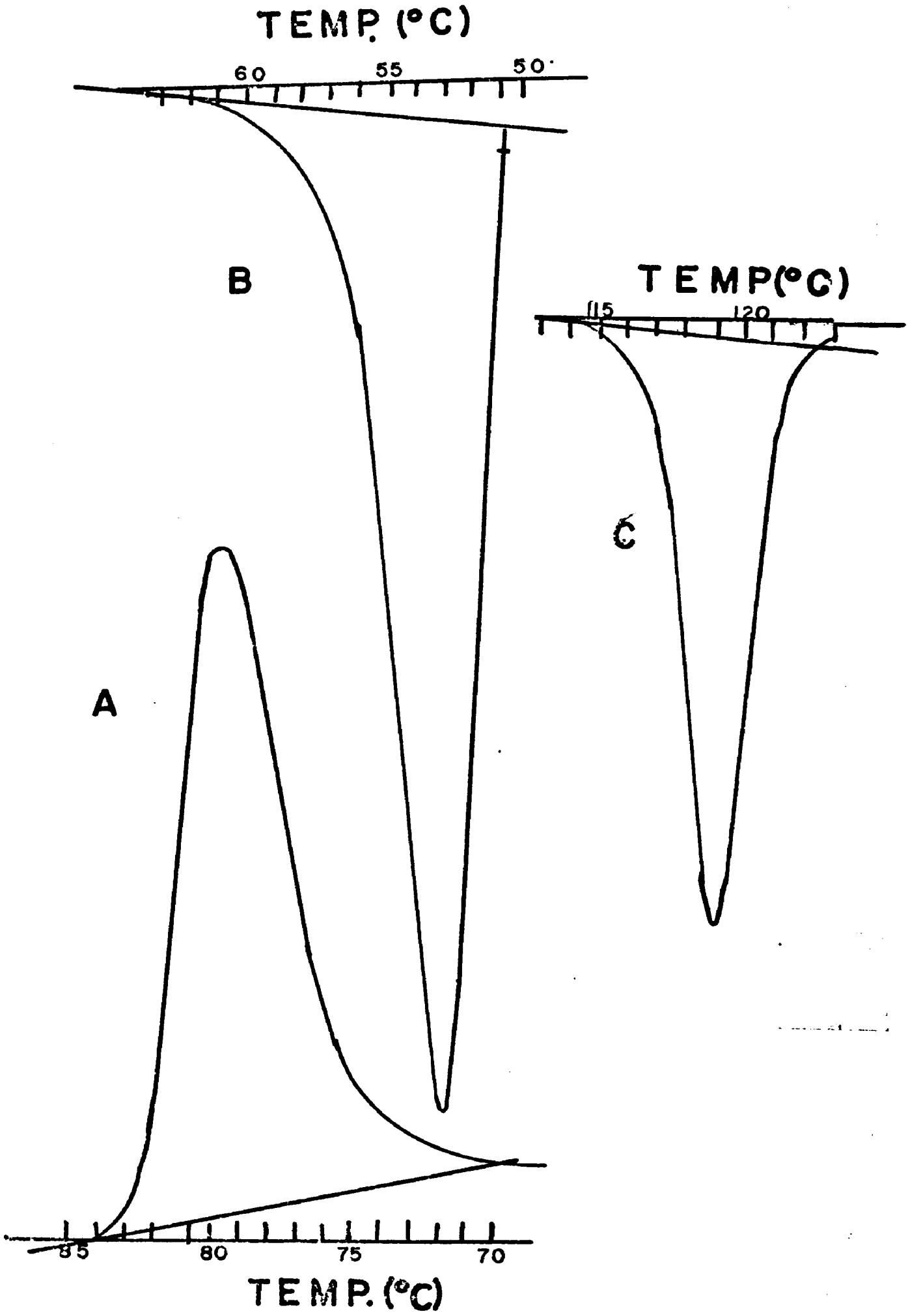
TEMP. (°C)
60
55
50
B
TEMP(°C)
115
120
C
A
85
80
75
70
TEMP. (°C)

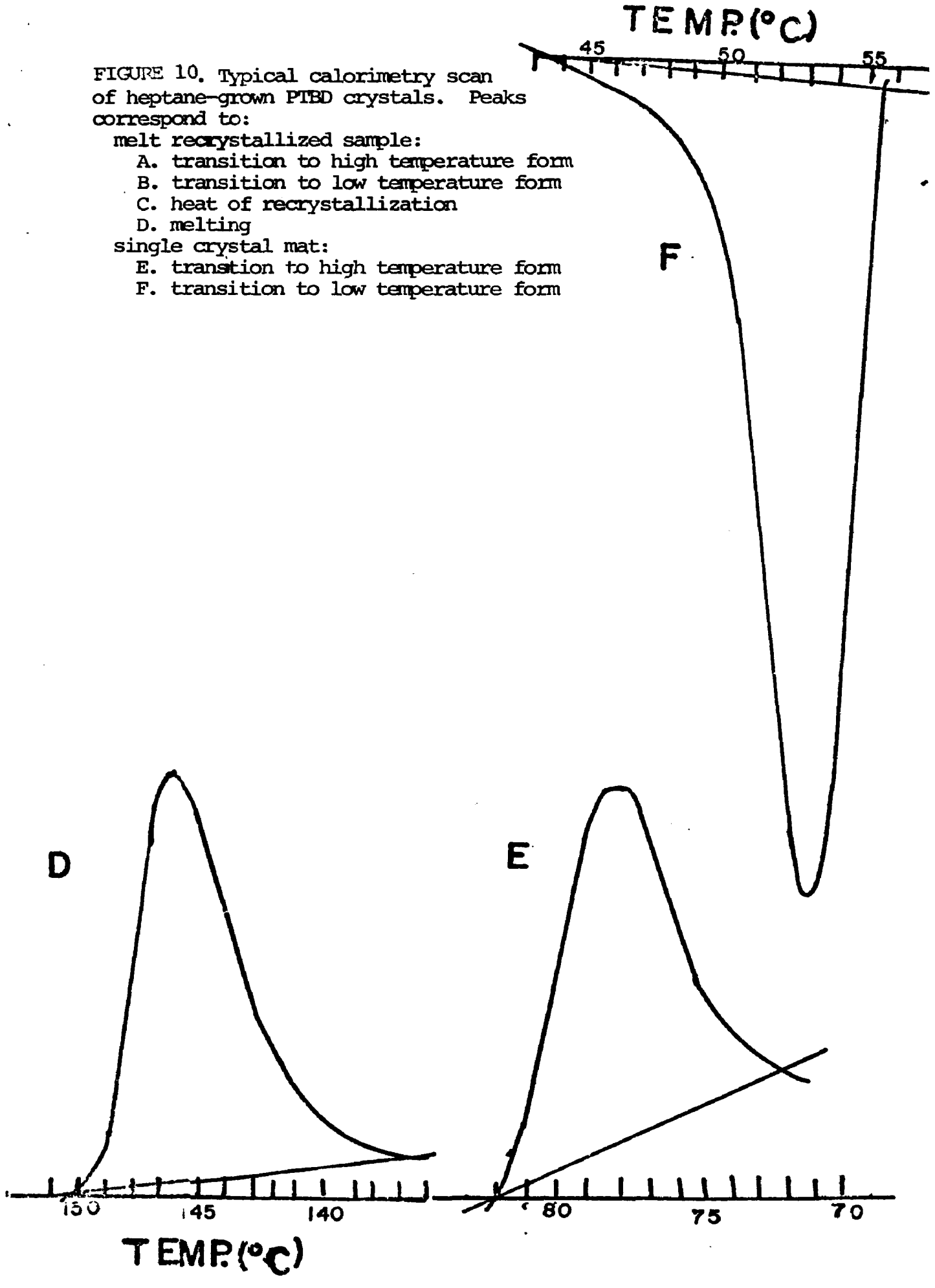

FIGURE 10. Typical calorimetry scan of heptane-grown PTBD crystals. Peaks correspond to:

melt recrystallized sample:

A. transition to high temperature form
B. transition to low temperature form
C. heat of recrystallization
D. melting

single crystal mat:

E. transition to high temperature form
F. transition to low temperature form

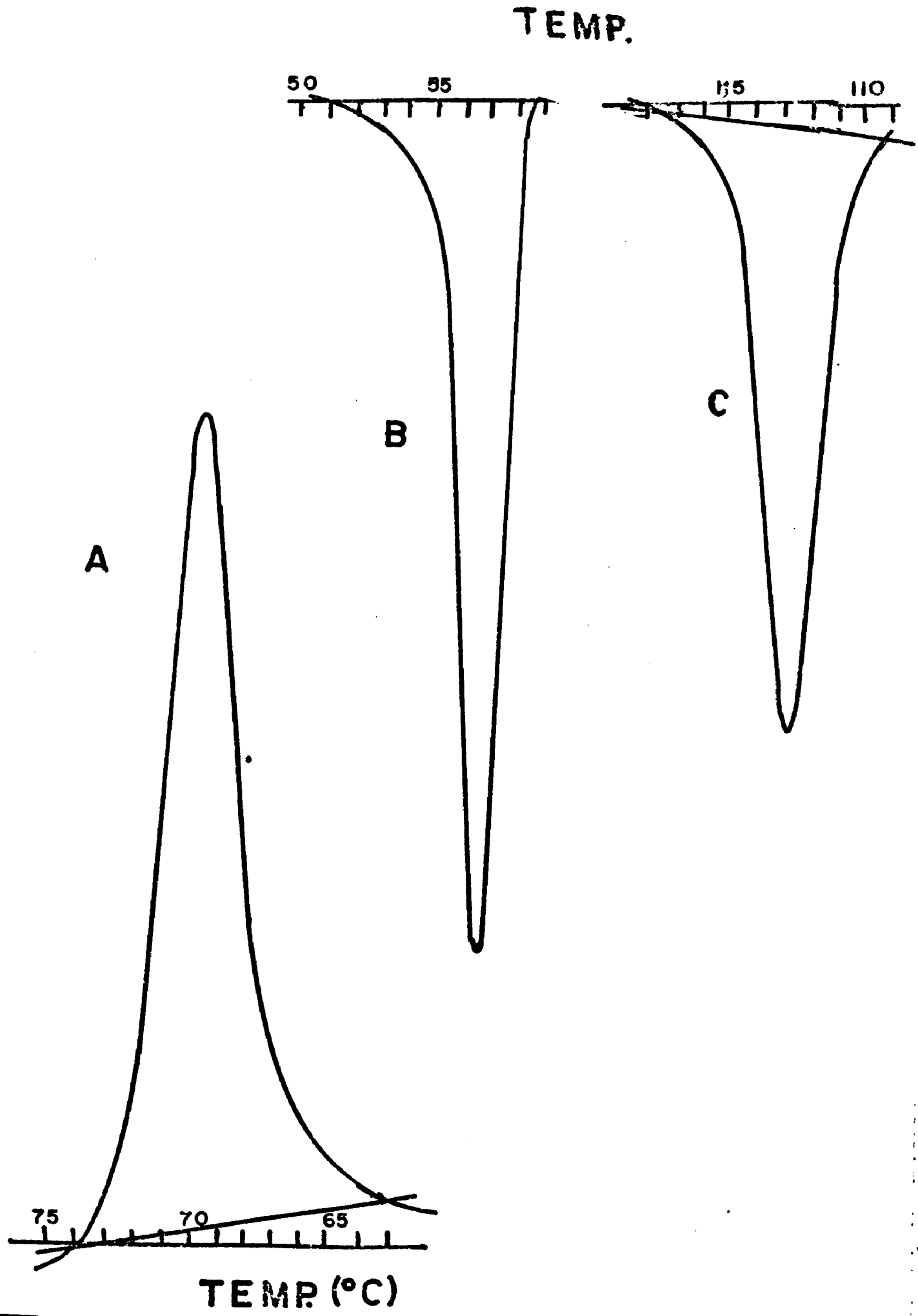
TEMP.
50
55
115
110
A
B
C
75
70
65
TEMP (°C)

FIGURE 11

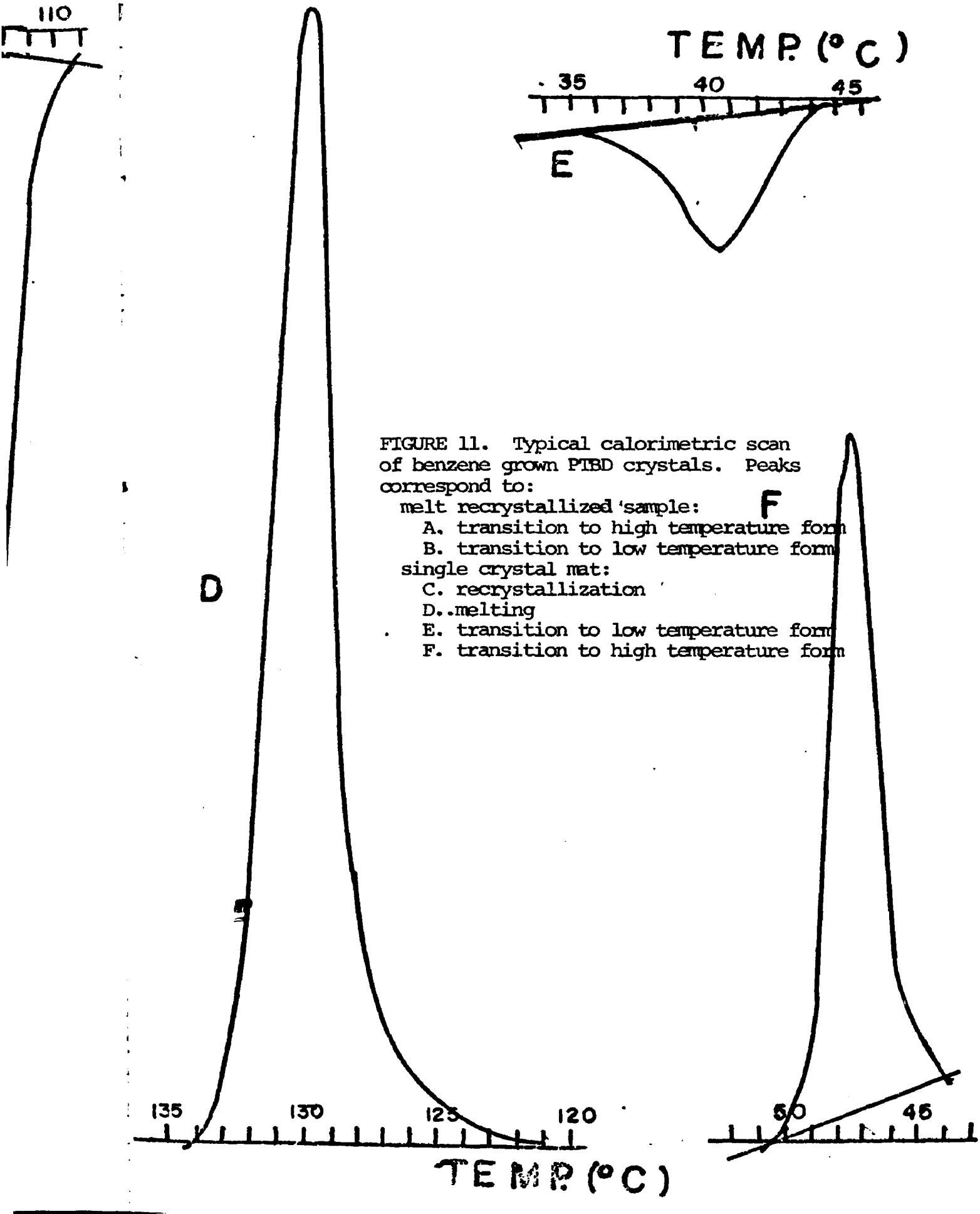

FIGURE 11. Typical calorimetric scan of benzene grown PTBD crystals. Peaks correspond to:

melt recrystallized sample:

A. transition to high temperature form
B. transition to low temperature form

single crystal mat:

C. recrystallization
D. melting
E. transition to low temperature form
F. transition to high temperature form

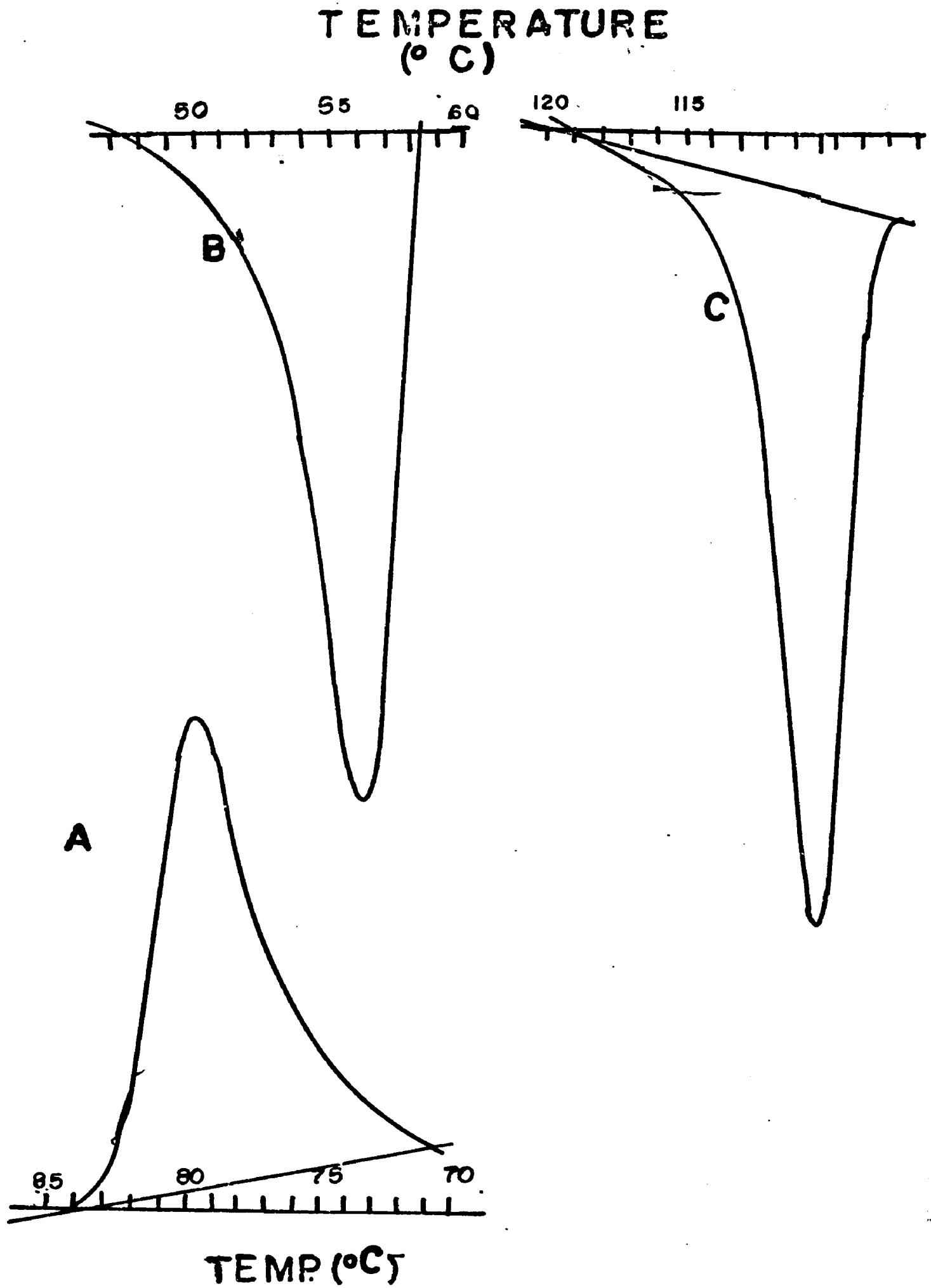
TEMPERATURE
(° C)
50
55
60
120
115
B
C
A
85
80
75
70
TEMP (°C)

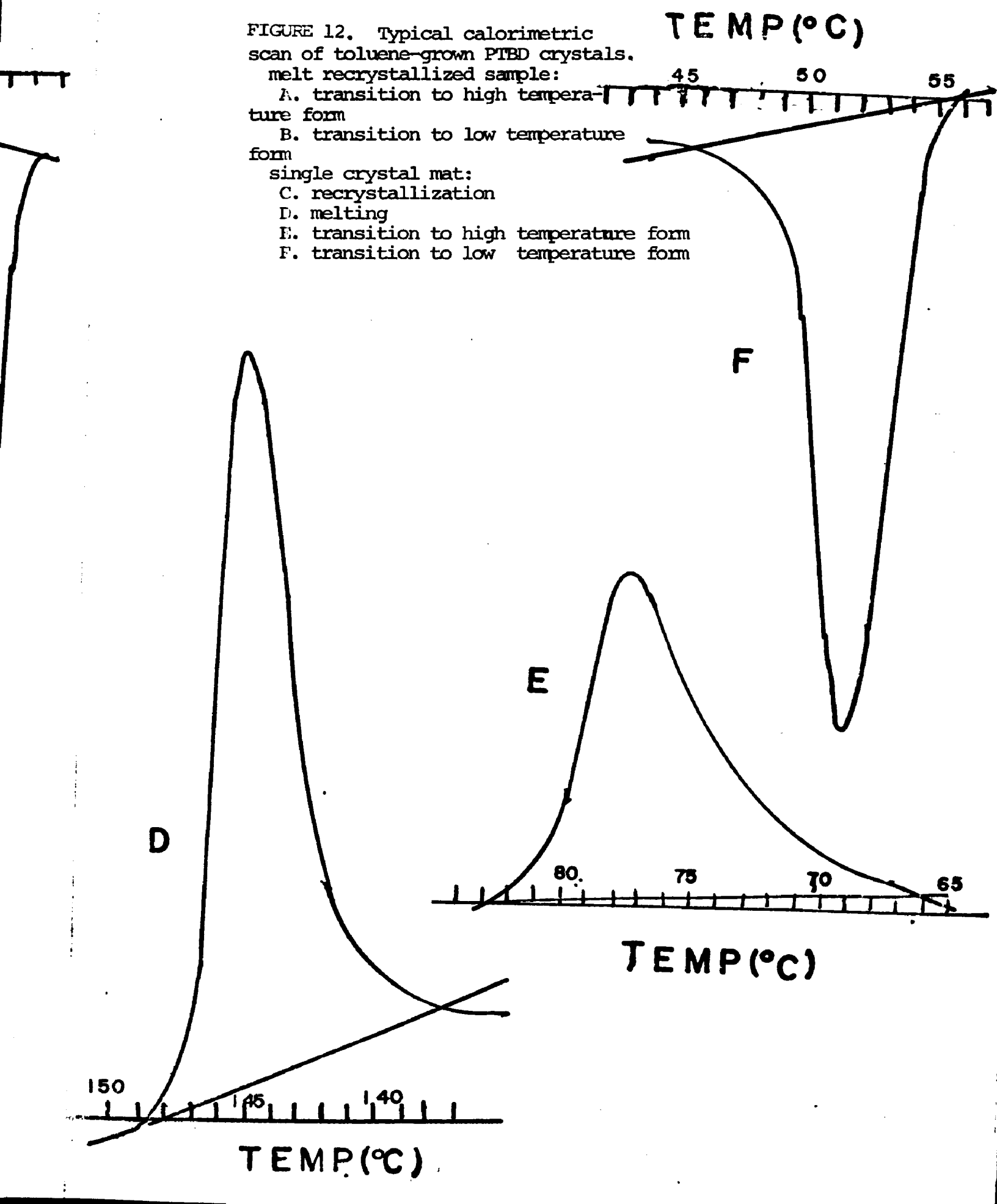

FIGURE 12. Typical calorimetric scan of toluene-grown PTBD crystals.
melt recrystallized sample:
A. transition to high temperature form
B. transition to low temperature form
single crystal mat:
C. recrystallization
D. melting
E. transition to high temperature form
F. transition to low temperature form

the doubling of the scan rate to affect the thermal behavior of the crystals. This did not happen. Finally, the scan of the irradiated toluene crystals, where lamellar thickening is suppressed, agreed well with the values obtained for the heat of transition of the unirradiated crystals. The radiation-induced cross-linking did, however, suppress the thickening of the melt recrystallized sample, which shows a lower heat of transition than all the other samples studied.

The heptane-grown single crystals all exhibited the highest degree of crystallinity and the greatest reproducibility of results. The transitional enthalpies of the melt-recrystallized sample were only 10% greater than the corresponding enthalpies for solution-grown lamellae. The crystals grown from benzene and toluene did not behave in this regular fashion, as can be seen from inspection of the error limits given in Table IV. The greater degree of amorphousness of these crystals is apparent both in the variability of their thermal behavior and in the large differences in the heats of transition of the single crystals and the melt recrystallized sample, 29% and 32% for benzene and toluene, respectively. However, once the samples were recrystallized from the melt, the enthalpy obtained was as reproducible as that for the heptane sample.

Another result indicative of the great degree of amorphousness of the toluene and benzene crystals is their temperature behavior. In addition to the fact that the transition temperature of the heptane crystals was higher than those of the toluene and benzene crystals, which average $55^{o}C$ and $65^{o}C$, respectively, it was also found that the transition temperature of

TABLE IV. Calorimetric Data for Crystals Grown from Various Solvents

Solvent	ΔH transition (cal/g)	ΔH melting (cal/g)	ΔH recrystall. (cal/g)	ΔH transition (melt recrystallized) (cal/g)
Heptane	27±1	15.3	15.7	26±1*
	26±2	16.5	14.2	28±2*
	24±2	16.4	14.2	27±2
Toluene	17±4	----	13.6	27±1*
	17±3	16.2	13.6	27±2*
	22±3	15.1	12.5	29±.5*
	18±3	14.5	14.5	27±2
Benzene	18±4	15.1	15.7	26±1*
	17±3	13.4	10.8	22±2
	19±5	13.1	13.7	30±4
Toluene (irradiated)	21±6	11.0	6.5	20±3

* Sample annealed near the transition temperature before the heats of transition were measured

the toluene and benzene crystals was not constant. The first few times a given sample underwent the transition, there was a rise in the transition temperature. The initial temperatures for toluene was 45°C and for benzene about 55°C. The same behavior occurred with the irradiated toluene sample, which indicates that the change was not due to thermal rearrangements. The effect is not attributable to solvent loss either, because there was no weight loss in the sample after thermal treatment. In addition, the transition peaks were all sharp and there was no rise in the peak area accompanying the rise in temperature. The areas all fluctuated around the mean values given in Table IV.

This behavior may be due to irreversible internal rearrangements which do not significantly contribute to the heats of transition. This irreversible rearrangement probably accounts for some of the non-reproducibility of the calorimetry results for the benzene and toluene crystals.

Table V summarizes the average enthalpies given in Table IV, and presents the entropies of the transitions and the temperatures, as well. As can be seen, the entropy of transition is greater than the entropy of melting, as was observed for the bulk polymer.[45] The entropies of all the melt-recrystallized samples are nearly identical. It also should be noted that for all three samples, the enthalpy, entropy and temperatures of melting and recrystallization, unlike those of the transition, agree quite well.

TABLE V. Calorimetric Data on Crystals Grown from Various Solvents

Averages of Runs Tabulated in Table IV

Solvent	Transition			Melting			Recrystallization			Transition (melt recrystallized sample)		
	ΔH (cal/g)	ΔS e.u.	^{o}C T	ΔH (cal/g)	ΔS e.u.	^{o}C T	ΔH (cal/g)	ΔS e.u.	^{o}C T	ΔH (cal/g)	ΔS e.u.	^{o}C T
Heptane	26±2	0.075	73	16.1±5	0.039	139	14.7±.6	.037	120	27±1	0.078	71
Toluene	19±3	0.058	55	15.3±.6	0.037	136	13.6±.5	.034	123	27±.3	0.078	71
Benzene	18±4	0.052	65	13.9±.8	0.034	135	13.4±2	.034	120	26±3	0.075	74

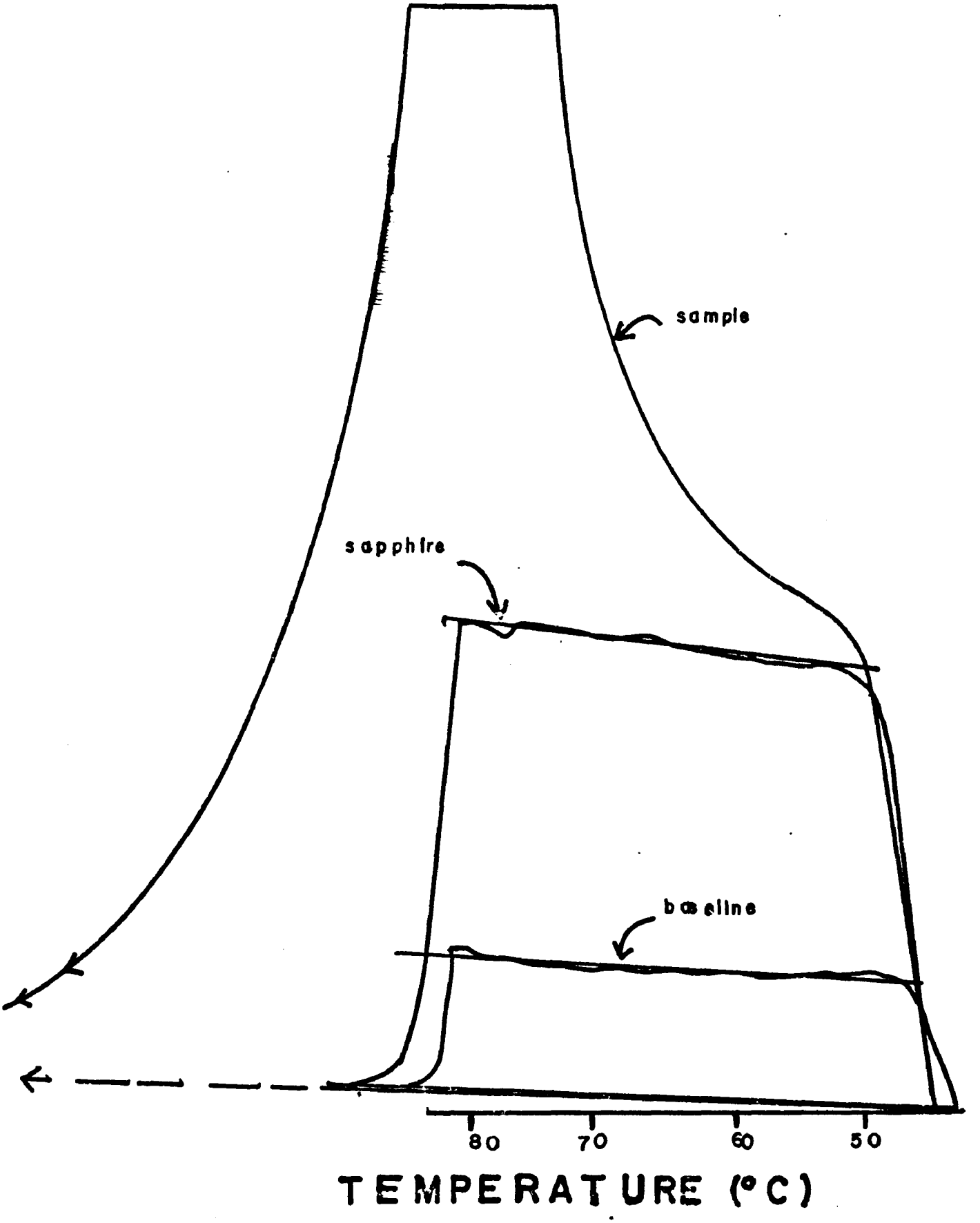

FIGURE 13 Specific heat scan of melt recrystallized PTBD between 45°C and 80°C, with sapphire standard and baseline superimposed.

FIGURE 14. Specific heat scan of melt recrystallized PTBD between 80°C and 110°C with sapphire standard and baseline superimposed.

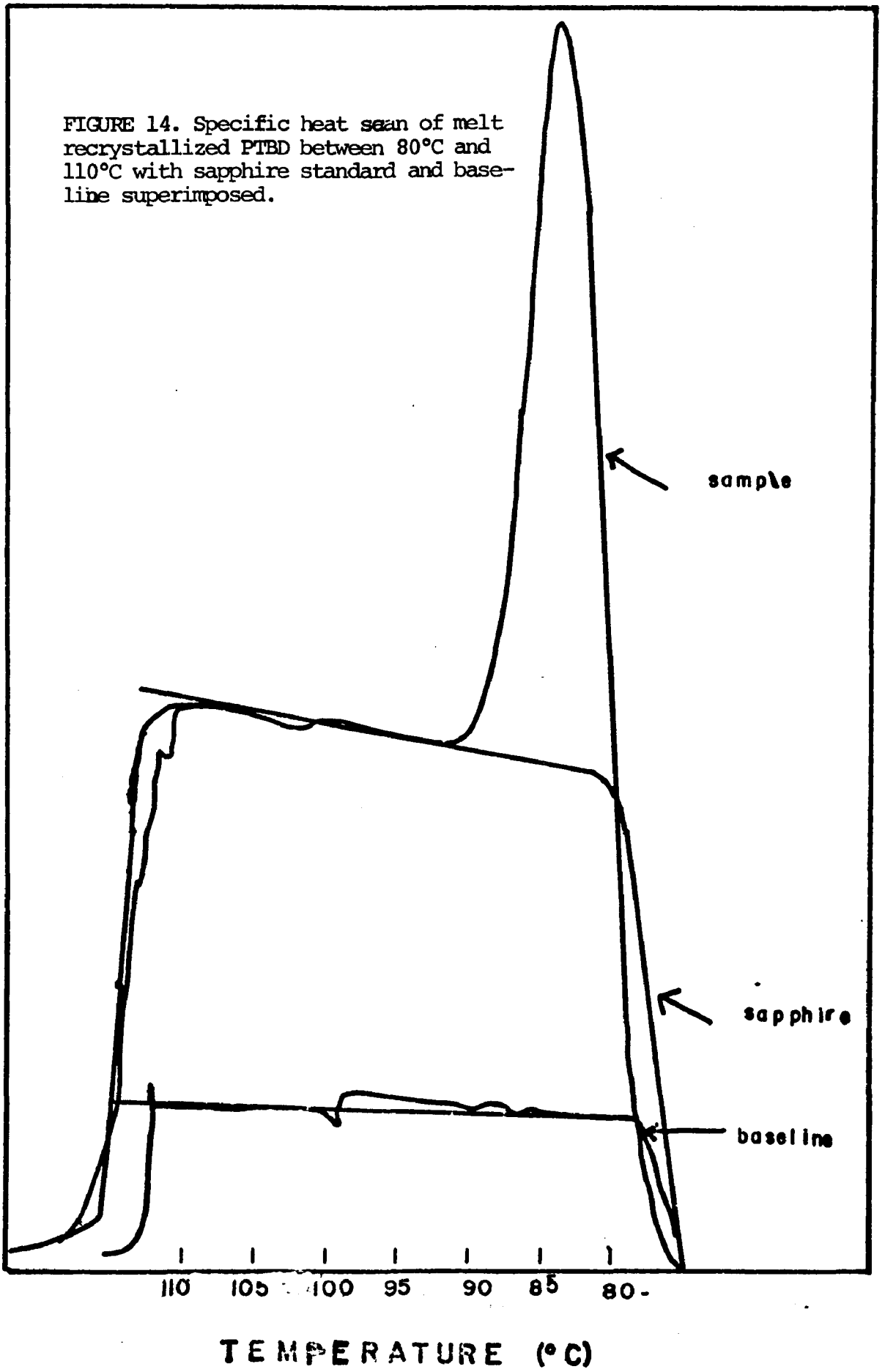

FIGURE 14

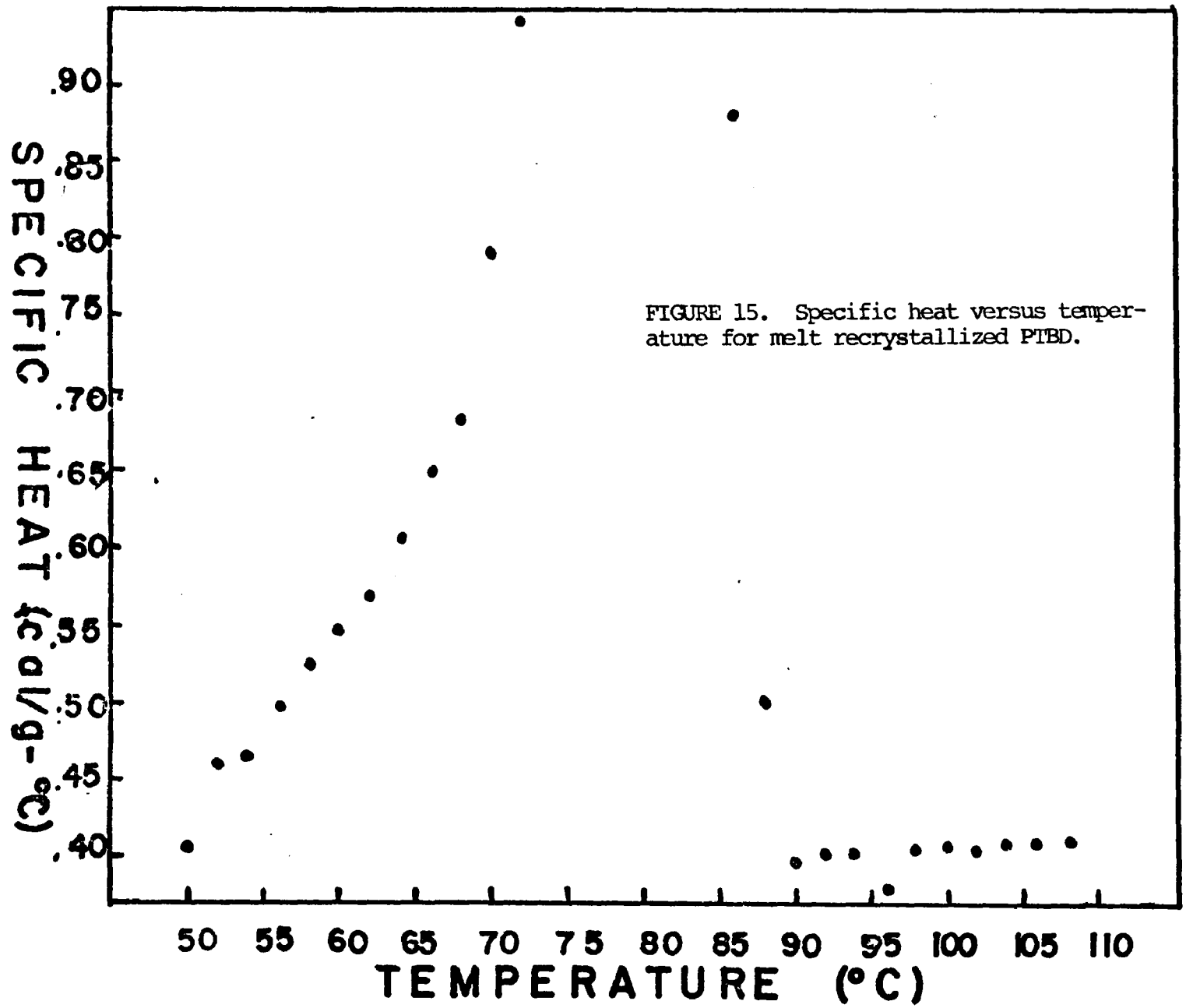

FIGURE 15. Specific heat versus temperature for melt recrystallized PTBD.

FIGURE 15

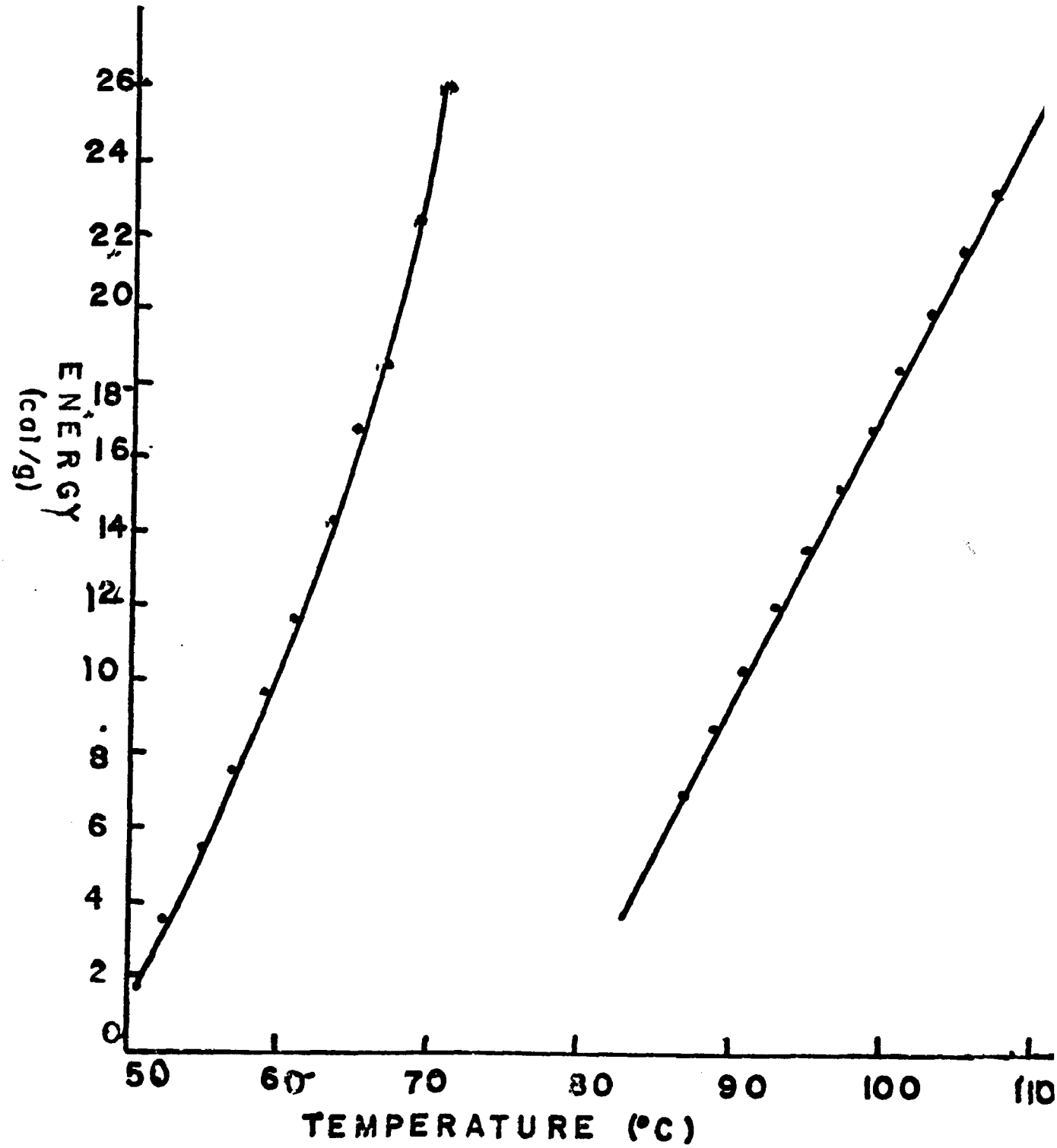

FIGURE 16

Numerical integral of specific heat versus temperature for melt recrystallized PTBD, with arbitrary zero of 50°C and 84°C for the low temperature and high temperature forms, respectively.

Specific heat measurments

The results of the last set of calorimetric experimetns appear in Figure 13-16. Figure 15 is a plot of the specific heat of melt recrystallized heptane crystals as derived from the experimental data in the manner described previously. Although several runs were made, only one set of results is plotted because a good baseline was not obtained for the sample in the other runs. The behavior of the peaks, however, was quite reproducible. In addition, the run was terminated at 110°C, again because the baseline did not re-establish within a reasonable time for useful extrapolation.

The heat capacity of the low temperature form rises rapidly towards infinity, up to the transition temperature, which is the characteristic behavior for a first-order phase transition. As the temperature increases beyond the transition, the heat capacity falls to a constant value until it approaches melting. Figure 15 is a plot of the numerical integral of the heat capacity curve. This is a plot of the energy of the crystal as a function of temperature. The reference temperature, t_o, for each form is the minimum temperature measured of that form. The energy changes of the low-temperature form are not linear, while the high temperature form lies exactly on a straight line , which indicates a constant heat capacity, ΔC_p.

DISCUSSION

The preceding results lead to a model for the structure of PTBD single crystals which is markedly dependent on the solvent and, therefore, the temperature of crystallization. The percentage of double bonds available for reaction, as well as the heats and temperatures of transition, indicate that heptane crystals grown near the transition temperature are more highly crystalline both in the interior and on the surface, than the benzene and toluene crystals, which are grown well below the transition temperature.

It is interesting to contrast the temperature and solvent behavior of PTBD to PE single crystals. Inspection of Table III reveals that the crystallization temperatures of benzene, toluene, and heptane crystals extend from 8°C. to 23° and 63°, respectively; yet the crystal thicknesses are essentially constant for all three preparations. Lamellar thicknesses of PE crystals, on the other hand, seem to be a more complex function of temperature and solvent.[13,34,69] Table VI shows the experimental results of Roe and Bair[13] for PE single crystals. They obtained 111 Å thick lamellae from both xylene and hexadecane with a temperature difference of only 7°C. As the temperature difference increased, large differences in lamellar thickness occurred.

Preliminary work with PTBD has indicated that crystals grown from heptane at 68°C. appear to have the same thickness as crystals grown at 63°C., indicating that PTBD lamellar thickness may be independent of crystallization temperature. R. St. J. Manley has reported similar behavior for amylose crystals.[69]

TABLE VI. Thicknesses of PE crystals Resulting from various preparations. [Data of Ref. 13]

Sample No.	T_c (°C.)	Solvent	l, Å
1	70	Xylene	104
2	77	Xylene	111
3	85	Xylene	126
4	90	Xylene	145
5	95	Xylene	178
7	84	Hexadecane	111
8	95	Hexadecane	125
9	100	Hexadecane	130
10	105	Hexadecane	154

The double bond titration results combined with the crystal thicknesses yield the average number of monomer units per surface fold. Division of the crystal thickness by the chain repeat distance of 4.83 Å [31] gives the number of monomer units in one traverse of a chain between the two fold surfaces of the crystal. Multiplication of this number of monomer units by the fractions of double bonds available yields the number of monomer units at all the surfaces per chain between the fold surfaces. By assuming that these reactive monomer units reside in folds, and that the amount in chain ends, tie molecules, and on the sides of the crystals is negligible, values of 3.2 to 6 monomer units per fold are obtained (Table III).

A calculation of the surface area of a hexagonal crystal 100 Å thick and 2μ on a side shows that the total area of six sides is only 0.05% of that of the two large faces, and indicates that the double bonds exposed on the crystal sides are negligible as compared to those at the two surfaces. Therefore,

for the n-heptane-grown crystals, and even for the smaller toluene-grown crystals, this area effect is negligible. For crystals with holes, a larger number of double bonds would be exposed, the amount depending on the number and size of the holes.

An estimate of the number of monomer units in nonreentrant chains (cilia) is obtained by dividing an average number of total monomer units in two cilia by the number-average degree of polymerization. The average length of cilia is taken as one-half the length of the chains in the body of the crystal between the fold surfaces.[26] For $\overline{M_n} \leq 11{,}000$, the number of monomer units in cilia is thereby calculated to be greater than or equal to 10%, and for $\overline{M_v} = 37{,}000$ it is calculated to be 3%. Using the first value to correct the number of monomer units per fold for the PTBD-U crystals and the second to correct those for the PTBD-K crystals yields the values for the corrected number of monomer units per fold given in Table III. In making these corrections, in addition to the assumptions above, it is further assumed that (1) the $\overline{M_n}$ of the PTBD-U chains in the crystals is equal to the $\overline{M_v}$ of the bulk material and (2) that $\overline{M_n}$ of PTBD-K crystals grown from toluene and MIBK is the same as that for crystals from n-heptane.

Thus, since a corrected value of 3 monomer units per fold is obtained for PTBD-U crystals, the increase in the percentage of double bonds available can be attributed to an increase in the number of cilia due to the decreased molecular weight of the polymer.

It is apparent from the experimental results that

PTBD-K crystals from MIBK have a greater number of available double bonds than those grown from either n-heptane or toluene. This greater number can be directly linked with the presence of holes in these crystals and the observed surface roughness which suggests a prevailing surface disorder (see Fig. 4).

A Surface Model

A comparison of the values of the number of monomer units per chain fold with the minimum number necessary to connect two adjacent chains in a crystal with the structure given for the low-temperature form of PTBD[31] is of interest for determining the relative tightness of the folds. The unit cell for the low-temperature form of PTBD is believed to contain four repeat units with the distance between units I and IV being larger than the other interchain distances by at least 50% (see Fig.18). Excluding the distance between units I and IV, the distance between units at the same elevation in the cellranges from 4.3 to 5.0 Å, which at the lower extreme is shorter than and the upper extreme is longer than the length of a repeat unit. Also a given atom in the repeat unit is not necessarily coplanar with the same atom in an adjacent chain. (See Figs.18a-c in Part II, where the crystal structure is discussed in greater detail.) Of the twenty possible connections between adjacent chains (ruling out I-IV) seven are found to include only one double bond and 13 to include two double bonds. It is therefore concluded that the average number of double bonds necessary for the tightest reentrant fold

will be between 1.5 and 2. Comparison of these values with those in Table III leads to the conclusion that reentrant folding for heptane-grown crystals is highly probable, although some fold looseness does occur. The crystals from toluene solution are less regular and titration results of Hendrix et al.[48] show that benzene-grown crystals are still more amorphous on the surface, with an average of 5 monomer units per fold.

Here again PTBD seems to be quite different from polyethylene. In their studies of the thermodynamic properties of PE single crystals, Sharma and Mandelkern[35], among others,[34,71] conclude that the only influence of solvent on structure is to relate the crystallization temperatures to a common undercooling, which yields different crystallite thicknesses. For the same crystallite size they find no direct solvent effect on the internal and interfacial structure. This is obviously not true for the interfacial structure of PTBD; as will be discussed shortly, the internal structure of PTBD crystals is dependent on the solvent.

Structure of the Crystal Interior

Many previous authors have associated amorphousness in single crystals predominantly with chain fold looseness[11,12] or with the presence of cilia.[26] In their study of the dynamical mechanical behavior and broad-line NMR of (1) PTBD mats grown from different solvents, and (2) mats undergoing the solid-solid phase transition, Tatsumi et al.[47] obtained results which could be attributed to (1) differences in the amorphous content

of the crystals arising from a change in growth solvent, or (2) from structural changes during the phase transition. They hypothesized that the solvent study results were due to differences in fold-tightness of the surface of the crystals grown from "good" and "bad" solvents, and that the changes observed upon the phase transition were due to fold-tightening which increased crystallinity.

This interpretation is questionable when considered in the light of results obtained in this study. When combined with the titration results, the data obtained from the scanning calorimetry experiments previously described indicate more crystal amorphousness than is present on the surface of the crystals alone, and specifically, that benzene and toluene crystals have significant amounts of internal defects in their crystal structure. The infra-red analysis of PTBD crystals of Hendrix et al.[48] also point to this conclusion. As previously discussed, techniques such as infra-red analysis and dynamical mechanical behavior cannot differentiate interfacial from interior defects. Therefore, care must be taken in the interpretation of data obtained from such experiments so that phenomena due to internal disorder in the crystals are not attributed to disorder of the interfacial surface.

The heats of transition and melting can be useful to further elucidate the crystal structure. Assuming that differences in enthalpy are due to different relative crystallinities of the samples, then the ratio of the measured heats to the relative crystallinities should a constant value. If the

heats are attributed to specific phenomena, such as fold-tightening, then division of these heats by the crystallinity changes resulting from these phenomena should lead to a constant value which would confirm the postulated mechanism. The relationship between the heats of transition, the surface amorphousness found by titration and the crystal amorphousness found from infrared analysis of Hendrix et al.[48] are shown in Table VII.

In Table VII, the amorphousness of the crystal surface (line 1) is assumed to be equal to the fraction of double bonds on the crystal surface as given in Table III and in Ref. 48. The amorphousness found by infra-red analysis (line 2) is not limited to the surface, but appears to include interior defects as well. The method of obtaining the amorphousness/crystalline ratio for PTBD is discussed in Ref. 48. The difference between the surface amorphousness and total crystal amorphousness should correspond to the amorphousness or internal defects in the crystalline interior of the crystals (line 3). It can be seen that the interior of a heptane crystal is highly crystalline, whereas the toluene and benzene crystals are quite defective. For toluene the interior is more defective than the surface, whereas the opposite is true for the benzene crystals. Further, since the ΔH_{tr} values of the benzene and toluene crystals are quite close (see line 4), whereas the surface amorphousness of these crystals is quite different, it is seen that the heat of transition cannot be attributed to differences in surface structure alone. When the

TABLE VII. RELATIONSHIP OF TRANSITION ENTHALPIES TO CRYSTALLINITY

	Solvents of Crystallization		
	Benzene	Heptane	Toluene
1. Amorphousness in surface region, from surface epoxidation, α_t	.27*	.14	.18
2. Amorphousness found by infra-red analysis, α_{IR}	.5*	.2*	.5*
3. Crystallinity in interior of crystals $\lambda_{int} = 1-[\alpha_{IR}-\alpha_t]$	.8	1	.7
4. ΔH_{tr} (cal/gram)	18±4	26±2	19±3
5. $\Delta H_{tr}/\lambda_{int}$	22±5	26±2	27±4

* Taken from Hendrix, Whiting and Woodward (reference 48)

heats of transition are divided by the interior crystallinities for the three samples, a relatively constant value is obtained, within the limits cited (see line 5, Table VII).

These results indicate that the differences in the calorimetric results observed during the transition are probably due more to differences in interior structure than differences in the surface. While the ΔH_{tr} for heptane and toluene differ markedly, the surface amorphousness does not. However, the interior of the heptane crystals is much more highly crystalline than the toluene crystals. Therefore the differences in the observed enthalpies are probably more justifiably attributed to these differences in the interior than to the interfacial structural differences.

It is probably reasonable to extend this conclusion to other techniques, such as dynamical mechanical properties. If one considers the percentage of the total crystal that surface defects represent, it is very reasonable to attribute the results to defects of the crystals as a whole, rather than to defects in their surfaces alone.

Effect of Growth Temperature

Finally, if we consider the specific heat data obtained from the melt recrystallized PTBD sample (Fig. 17), we can begin to understand why the differences in interior structure of crystals grown from various solvents arises. A rising heat capacity indicates that the polymer can occupy higher energy states corresponding to the higher energy conformations of the

chains. One sees that the high temperature form of PTBD has a constant heat capacity. This constancy can be interpreted as indicating that the polymer has so much conformational freedom in its crystal structure that all available conformational states are occupied and the heat capacity would therefore not change

When one compares the measured entropy of transition to the entropy of melting (see Table V), one sees that ΔS_{tr} is much greater than ΔS_m, which further verifies this hypothesis, since increase in the structural randomness of the crystals entering the high-temperature form is much greater than the increase of randomness in going from the high-temperature form to the melt. This means of course, that the high temperature form is a highly disordered crystalline form. This is also the explanation of the fact that X-ray studies of the high temperature form yielded only average interchain distances rather than specific lattice constants.[31] The motion of the chains is so great that a distinct pattern cannot be obtained.

In light of these arguments, if one looks at the growth temperatures of the benzene and toluene crystals in comparison to the growth temperature of the heptane crystals, one finds that the heptane crystals are grown very close to the solid-solid transition temperature, whereas the benzene and toluene crystals are grown well below the transition temperature.

The results suggest that at the temperature at which heptane crystals are grown considerable torsional motion is present in the chains; either before or upon cooling down to

room temperature, considerable internal ordering can apparently take place. However, for crystals grown well below the transition temperature, it appears that amorphous conformations are included in the crystal interior. When these crystals are melted and recooled, the ordering can be improved, leading to closer agreement in the thermodynamic properties for all crystal preparations.

The differences in interfacial structure may also partially depend on the precipitation temperature, but they could also be due to the differences in solvation. No experimental work was conducted on the equilibrium dissolution temperature of PTBD in each of the solvents used, so the relative amount of undercooling for each of these systems is not really known. Before one postulates a solvent effect of the surface, such equilibrium temperature experiments must be performed.[35] However, the experiments described here quantitatively indicate that differences in internal and interfacial structure of PTBD crystals grown from various solvents at different temperatures do exist.

CONCLUSION

By chemically reacting the exposed double bonds on the surface of PTBD crystals, it is found that crystals grown from different solvents, and crystals from different molecular weight polymers, have various amounts of double bonds available for reaction. Calorimetric studies showed that the interior structure of the crystals is a function of solvent and growth temperature as well.

Crystals grown from n-heptane at a temperature near the transition point were found to be highly crystalline (80-90%) with a regularly re-entrant surface structure. This is believed to be due to the large amount of conformational freedom available to the polymer at this growth temperature. Crystals grown from benzene and toluene well below the transition temperature were found to be highly defective (50% crystalline), probably due to the inclusion of amorphous conformations within the crystal lamellae. The surface of the benzene crystals is quite amorphous while the toluene crystals seem to have a surface structure which is fairly regular but with some amorphousness present.

Since the titrations, which are an experimental measure of surface structure alone, show relative amorphousness which differs from the calorimetric result, it is seen that it would have been erroneous to attribute all thermodynamic differences to differences in interfacial structure. Conclusions about surface structrure cannot be drawn from techniques which measure

the properites of the entire crystal, especially in light of the experiments described here and those of Hendrix, Whiting, and Woodward[48] which indicate the presence of internal defects as a function of growth temperature and solvent.

PART II

INTRODUCTION

One of the major problems encountered in performing theoretical calculations is the difficulty of doing theoretical "experiments" which can be compared to a laboratory experiment without the use of drastic approximations. For example, consider the approximations necessary in the prediction of the heat of melting of a polymer. Since the heat of melting requires comparing the energy of the melt to the energy of the solid, one must describe the geometrical structure of the melt. An exact mathematical description is not possible at present. A popularly used approximation is to postulate that the chain assumes an all-trans conformation in the melt. Generally the energy of the melt is then considered to be the energy of a single all-trans chain.

With PTBD, however, many of these approximations can be avoided. Since PTBD undergoes a solid-solid phase transition between two forms for which experimental and structural data are available[31,32], theoretical calculations of transitional energies can be made which are not based on assuming an all-trans or any other hypothetical conformation for the polymer. PTBD thus provides a system for testing energy functions and single-chain approximations commonly used by workers in the field.

There are several open questions concerning the formulation of theoretical energy functions. One is the form of the energy functions used, and the representation of contributions to the energy by chain motions and lattice vibrations. Torsional contributions

are generally represented as a constant factor, the magnitude of which is determined by the torsional angles of the molecule. Since the lattice dimensions of PTBD as a function of temperature are known[32], the potential energy can be calculated as a function of distance and can be compared to the energy obtained from heat capacity measurements. The difference between the two can be used as an estimate of the torsional modes.

A second important question which can be studied with PTBD is the use of single-chain energy calculations for describing the energy of a crystalline system. The calculations to be described here are based on a lattice of 125 contiguous, identical unit cells. The energy minima and the lattice dimensions and chain orientation at these minima can be compared for the single chain, the unit cell and the entire lattice. Since the single-chain intramolecular calculations occupy such a large part of the literature, this study should provide a critical evaluation of those calculations.

The Energy Function Problem

In order to describe a physical system mathematically, or to calculate parameters of a system theoretically, one must have an energy function which accurately describes the system. However, since most real systems cannot be treated exactly, it becomes necessary to derive equations based on reasonable approximations and simplifications. Specifically, in molecular energy calculations, energy functions must be "parameterized" in some way to fit experimental data. There are probably as many sets of para-

meters as there are workers in this field. One reason for this is that experimental data available do not, for the most part, describe single molecules. Thermodynamics, for instance, is a science which specifically seeks to represent extremely complicated systems in terms of a few specific macroscopic parameters. Unless one is working with small molecular systems where energies can be evaluated by such techniques as infrared spectroscopy, one has to rely heavily on thermodynamics for experimentally determined energies.

The problem of finding a suitable energy function can be partially resolved, however, because precise experimental data on molecular geometry is available. Since the potential energy is a function of distance, r, the distance dependence of the energy function need not be approximated. The form of the function will depend on the nature of the interactions and the way they are described.

There are two popular methods of approaching the problem of describing the energetics of a polymeric system. The first is based on mathematical representations of rotational isomeric states. One can consider the ethane molecule, for example, as existing in two or more conformational states, separated by energy barriers. Each of these states or conformers can be thought of as in an energy well which is mathematically representable as a cosine function. This approach, developed predominantly by Volkenshtein[56] and Flory[57] is to assign Boltzmann weights to chosen configurations around successive bonds. These are calculated as a function of the probability that the molecule will be in the particular conformation, which is, of course, a function of the energy assigned to each state.

Once these Boltzmann factors are specified, the partition function of the system can be calculated by an evaluation of the configuration integral of the system. This calculation is performed using matrix methods. The mechanics of this particular method will not be discussed in great detail because it was not used in this study.

The aforedescribed method has been applied to PTBD by Mark[49,50] and Abe and Flory[52], as well as Corradini[46]. The rotational states chosen were based on studies of propylene and the authors then attempted to compare solution properties of PTBD obtained from single-chain calculations to experimentally derived values. The conclusion reached by Mark was that a lattice calculation was essential in order to estimate the validity of the intramolecular calculations. The interpretation of the other results obtained in those studies cannot be readily applied to the solid crystalline state.

An alternative approach to the energy function problem is the one largely developed by Scott and Scheraga in a series of papers[58-63] and is the approach utilized here. This point of view is that when stereoregular polymers crystallize, they assume the conformation which achieves the minimum free energy of the system. Scott and Scheraga postulated an intramolecular potential energy function and used parameters obtained by fitting to the relative energies of conformers obtained by spectroscopic studies. The parameterized functions were then used in a "computer seach" for the particular conformations which achieve the minimum energy.

The conformational energy is computed by a number of schemes which have been predominantly associated with the work

of Wiberg[62], Hendrickson[63], Allinger[64], Westheimer[65] and their various co-workers. The Scott and Scheraga technique is another variation of the basic scheme. In these methods, the total conformational energy, U, is considered to be a sum of the energy due to non-bonded interactions (interactions among all the atoms not covalently bonded), U_{nb}, and the torsional energy (energy due to the ethane-like rotational barriers in the molecule), U_{tors}.

$$U = U_{tors} + U_{nb} \qquad (3)$$

The exact choice of the potential functions varies but the two most popular forms for U_{nb} are the Buckingham potential (4) and the Lennard-Jones (γ,δ) potential, (5), where a, b and c are adjustable

$$f(r) = ar^{-6} + b \exp(-cr) \qquad (4)$$

$$f(r) = ar^{-\gamma} + br^{-\delta} \qquad (5)$$

parameters and γ and δ are small positive integers, often 6 and 12.

Two functions were used in this study. One was the Scott and Scheraga function and the second was the energy function derived by Kitaigorodsky and others[66,67], which was parameterized from the Van der Waals radii collected from crystal lattice data. The Kitaigorodsky function was used in the calculations of the heat capacity because it was found to reproduce the lattice dimensions extremely well at the energy minimum of the low-temperature form.

The Kitaigorodsky function is of the Buckingham potential type and does not consider the lattice energy separately. The Scott and Scheraga function does treat the U_{tors} separately. They "chose"

a sinusoidal potential function (6), where V_o is assumed to be a constant for a given series, and ω_i are the dihedral angles (the angles defining the planes between adjacent atoms) of the molecules.

$$(6) \quad U_{tors_i} = \frac{V_o}{2} \left(1 + \cos(3\omega_i) \right)$$

EXPERIMENTAL

The "experimental" section will consist of a mathematical description of the geometry of a chain, the generation of the initial chain coordinates, and the geometric relationships and transformations used to produce a unit cell and then a lattice of cells. This will be followed by a description of the various computer experiments performed on these generated systems.

Geometry of a Chain

The main geometrical parameters of PTBD are shown below.

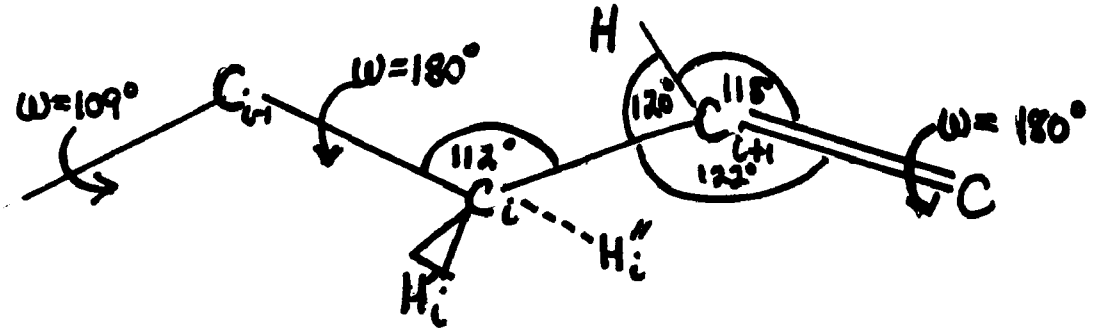

Definition of structural parameters

The relevant parameters are defined as follows, where the values of the angles are based on the experimentally determined structure:

$$\theta_i = \angle C_{i-1}C_iC_{i+1} = 112^o$$

$$\alpha_i = \angle H'_i\, C_iH''_i = 109.28^o$$

$$\delta = \angle H''_iC_iC_{i-1} = \angle H'_iC_iC_{i+1} = \angle C_{i-1}C_iH'_i \pm 108.5^o$$

$\gamma = \cos[(\cos\delta - \cos\delta\cos\theta_i)/\sin\delta\sin\theta_i]$ = projection of the angle δ onto a plane through C_i and perpendicular to the bond $C_{i-1}C_i$

Table VIII. gives the other structural parameters used in this study.

TABLE VIII. Structural Parameters for PTBD

-C-C-	= 1.54 Å	-C=C-	= 1.32 Å
-C-H-	= 1.08 Å	≡C-H-	= 1.08 Å

Generation of Initial Coordinates

The initial coordinates are generated according to the local-global transformation scheme first used by Eyring.[68] In this scheme we fix a local coordinate system on every backbone atom, according to the conventions illustrated below. We let the

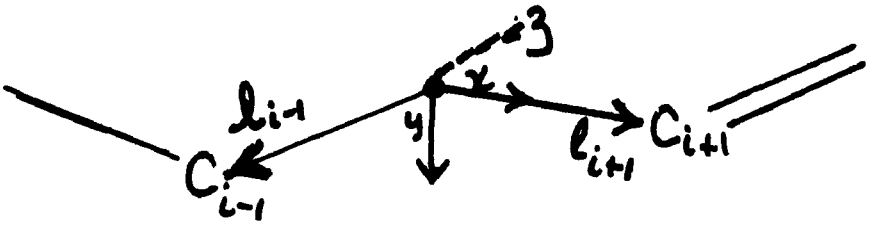

Local coordinate system of C_i

local x-axis of the i^{th} atom coincide with the bond vector $\vec{I}_i$, connecting atoms i and i+1. The local y-axis lies in the plane formed by atoms i-1, i, and i+1, making an acute angle with the bond vector $\vec{I}_{i-1}$. The z-axis is chosen to make a right-handed coordinate system with the x- and y- axes. A laboratory frame of reference, O, is taken to coincide with the local coordinate system of atom 1.

Now, using the Scott and Scheraga transformation scheme[58] for constructing a polymer with a given set of dihedral angles, we do the following operations. Transform the coordinates of a given carbon atom to the frame of reference of the previous backbone atom and continue to do so until it is finally described in the laboratory frame of reference, the local coordinates of the first atom. Specifically, the coordinates of the carbon atom and two hydrogen atoms attached to a given carbon, C_i, in the frame of reference of atom C_{i-1}, are represented by the following 3 x 1 column vectors:

$$(7)\quad \vec{\chi}_{C_i}(C_{i+1}) = \begin{bmatrix} \ell_i \\ 0 \\ 0 \end{bmatrix}, \quad \chi_{C_i'}(H_i') = \begin{bmatrix} \ell_i' \\ 0 \\ 0 \end{bmatrix},$$

$$\vec{\chi}_{C_i''}(H_i'') = \begin{bmatrix} \ell_i'' \\ 0 \\ 0 \end{bmatrix}$$

Examination of the local coordinate system illustrated above will show that since the origin is located at the C_i carbon atom, the length of the vector separating the two atoms in the x direction describes the location of the atom in this coordinate system.

Scott and Scheraga developed a set of transformation matrices and vectors which perform the necessary geometric maneuvers for this coordinate transfer. The mathematical operations performed are given by:

$$(8)\quad \vec{\chi}_{C_{i-1}}(C_{i+1}) = \underset{\sim}{T}_{i \to i-1}\, \vec{\chi}_{C_i}(C_{i+1}) + \vec{t}_{i \to i-1}$$

$$\vec{\chi}_{C_{i-1}}(H_i') = \underset{\sim}{T}'_{i\to i-1}\,\vec{\chi}'_{C_i'}(H_i') + \vec{t}_{i-i-1}$$

(8)

$$\vec{\chi}_{C_{i-1}}(H_i'') = \underset{\sim}{T}_{i\to i-1}\,\vec{\chi}_{C_i''}(H_i') + \vec{t}_{i\to i-1}$$

The $\underset{\sim}{T}$'s are transformation matrices for the coordinate systems located on adjacent atoms and the $\vec{t}$'s are vectors for the corresponding translations along the chain.

Equations (9a) are the transformation matrices for sp^3 hybridized carbon atoms.

$$\underset{\sim}{T}_{i\to i-1} = \begin{bmatrix} -\cos\theta_i & -\sin\theta_i & 0 \\ \sin\theta_i\cos\omega_i & -\cos\theta_i\cos\omega_i & -\sin\omega_i \\ \sin\theta_i\sin\omega_i & -\cos\theta_i\sin\omega_i & \cos\omega_i \end{bmatrix} \quad (9a)$$

$$\underset{\sim}{T}'_{i\to i-1} = \begin{bmatrix} -\cos\delta & -\sin\delta & 0 \\ \sin\delta\cos(\omega_i+\gamma) & -\cos\delta\cos(\omega_i+\gamma) & -\sin(\omega_i+\gamma) \\ \sin\delta\sin(\omega_i+\gamma) & -\cos\delta\sin(\omega_i+\gamma) & \cos(\omega_i+\gamma) \end{bmatrix}$$

$$\underset{\sim}{T}''_{i\to i-1} = \begin{bmatrix} -\cos\delta & -\sin\delta & 0 \\ \sin\delta\cos(\omega_i-\gamma) & -\cos\delta(\cos\omega_i-\gamma) & -\sin(\omega_i-\gamma) \\ \sin\delta\sin(\omega_i-\gamma) & -\cos\delta\sin(\omega_i-\gamma) & \cos(\omega_i-\gamma) \end{bmatrix}$$

The corresponding matrics for sp^2 hyrbridized carbon are:

$$\underset{\sim}{T}_{i \to i-1} = \begin{bmatrix} -\cos 122^\circ & -\sin 122^\circ & 0 \\ -\sin 122^\circ \cos\omega_i & -\cos 122^\circ \cos\omega_i & \sin\omega_i \\ \sin 122^\circ \sin\omega_i & \cos 122^\circ \sin\omega_i & \cos\omega_i \end{bmatrix} \tag{9a}$$

$$\underset{\sim}{T}'_{i \to i-1} = \begin{bmatrix} 1/2 & -\sqrt{3}/2 & 0 \\ \sqrt{3}/2 \cos\omega_i & -1/2 \cos\omega_i & \sin\omega_i \\ -\sqrt{3}/2 \sin\omega_i & -1/2 \sin\omega_i & -\cos\omega_i \end{bmatrix} \tag{9b}$$

The translations vectors are given by (10).

$$\vec{t} = \begin{bmatrix} l_i \\ 0 \\ 0 \end{bmatrix} \tag{10}$$

The generation of a complete chain now consists of incrementing the chain index, i, and seeing what atom of the monomer unit it corresponds to. This defines the proper bond angles and distances to be used in(9) and (10). Then, one by one, the coordinates of each atom are calculated in the laboratory frame and computed as an iterated matrix product. The laboratory frame coordinates of the (i+1)st backbone atom are given by (11).

$$\vec{\chi}_i(i+1) = \left[\prod_{k=2}^{i} \underset{\sim}{T}_{k \to k-1}\right] \vec{\chi}_i(i+1) +$$

(11)

$$\left[\prod_{k=2}^{i-1} \underset{\sim}{T}_{k \to k-1}\right] \vec{t}_{i \to i-1} +$$

$$\left[\prod_{k=2}^{i-2} \underset{\sim}{T}_{k \to k-1}\right] \vec{t}_{i-j+2 \to i-j+1} \quad \cdots\cdots$$

$$+ \vec{t}_{2 \to 1}.$$

Generation of a Unit Cell

The first three atoms of the generated chain, which define the laboratory coordinate system, lie in the x-y plane, with H_1 at the origin. Rather than redefining the coordinate system to match the geometry of the unit cell, the chain was reoriented in space to achieve this result. First, it is rotated up so that the line bisecting the midpoint of each double bond coincides with the z-axis of the laboratory frame of reference. Then, since the crystal structure is monoclinic, the a-axis is not orthogonal to the c-axis and therefore the chains must be tilted. Specifically, an examination of a model of PTBD shows that this tilt is equivalent to having the projection of the double bond bisector be at an angle of 225° in the x-y plane.

Once the chain has been rotated to this position, it is then duplicated at the appropriate lattice sites or at specific

interchain distances in a hexagonal lattice. Chains II and III are not identical to I and II, however, as is illustrated in Figure 17, because corresponding atoms on the chain are not coplanar. Therefore, before chain III is copied from chain I it must be translated. The following transformations and equations were used in the generation of the unit cell:

1. Rotating the initial chain so that the line bisecting the double bonds coincides with the z-axis of the laboratory frame:

(a) [Referring to Figure 18a] translation to have midpoint of first double bond at the origin by finding the midpoint of the coordinate of the double bond and subtracting these coordinates from every other coordinate.

(b) [Referring to Figure 18a] rotation of chain through angle of the vector v, connecting the midpoint of the double bonds.

2. Tilting the chain at the proper angle:

(a) Finding the current orientation of the double bond

(12)
$$\cos\omega = x_4/(x_4^2 + y_4^2)$$
$$\sin\omega = y_4/(x_4^2 + y_4^2), \text{ where } \omega = \text{current orientation angle}$$

and x_4 and y_4 are the coordinates of C_4 in the monomer unit

(b) Transforming to 225° orientation

(13)
$$\text{all } x' = x(\cos 225^\circ \cos\omega + \sin 225^\circ \sin\omega) - y(\sin 225^\circ \cos\omega - \cos 225^\circ \sin\omega)$$
$$\text{all } y' = y(\cos 225^\circ \cos\omega + \sin 225^\circ \sin\omega) + x(\sin 225^\circ \cos\omega - \cos 225^\circ \sin\omega)$$
$$\text{all } z' = z = \text{unchanged}$$

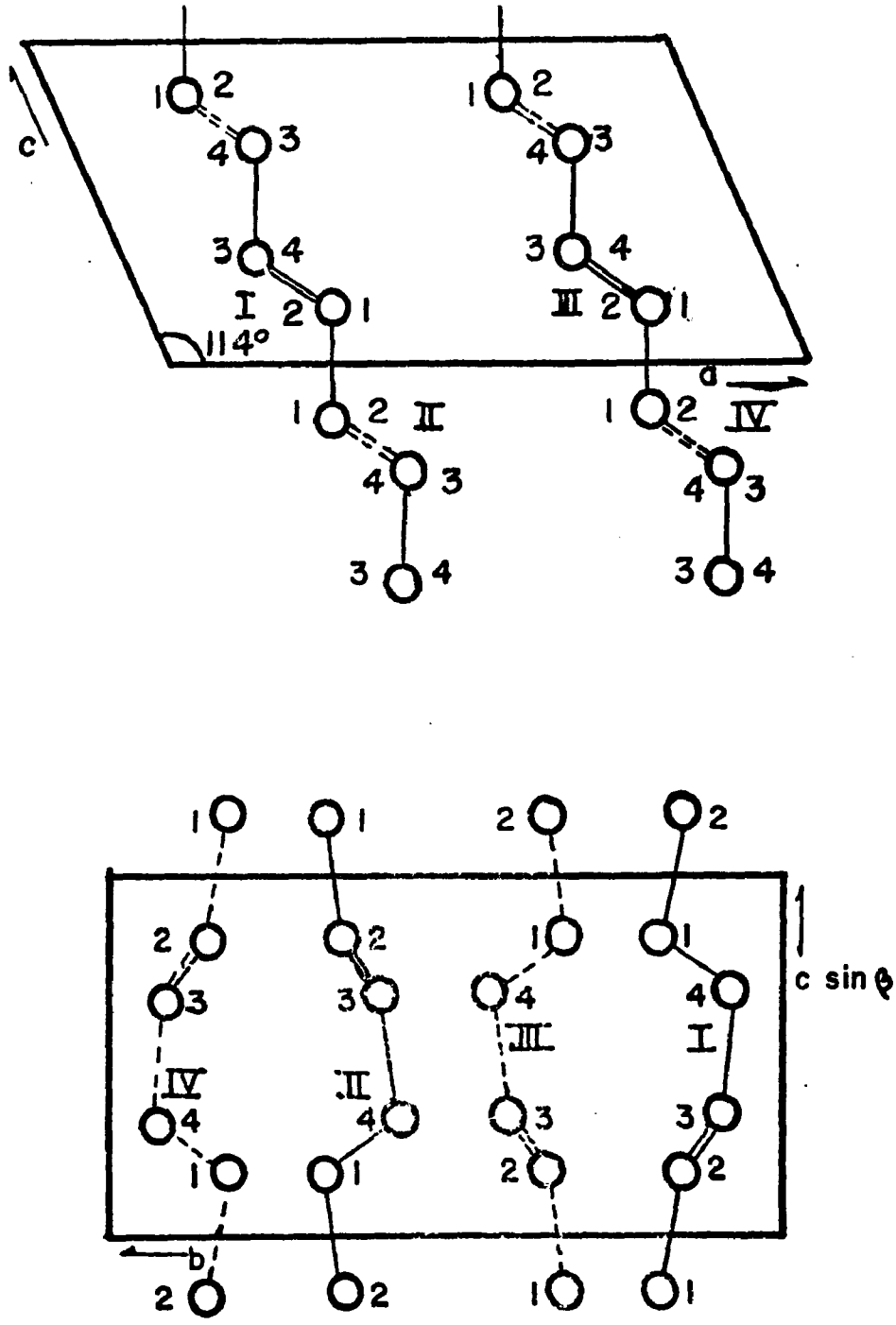

FIGURE 17
Crystallographic structure of PTBD, taken from reference 31.

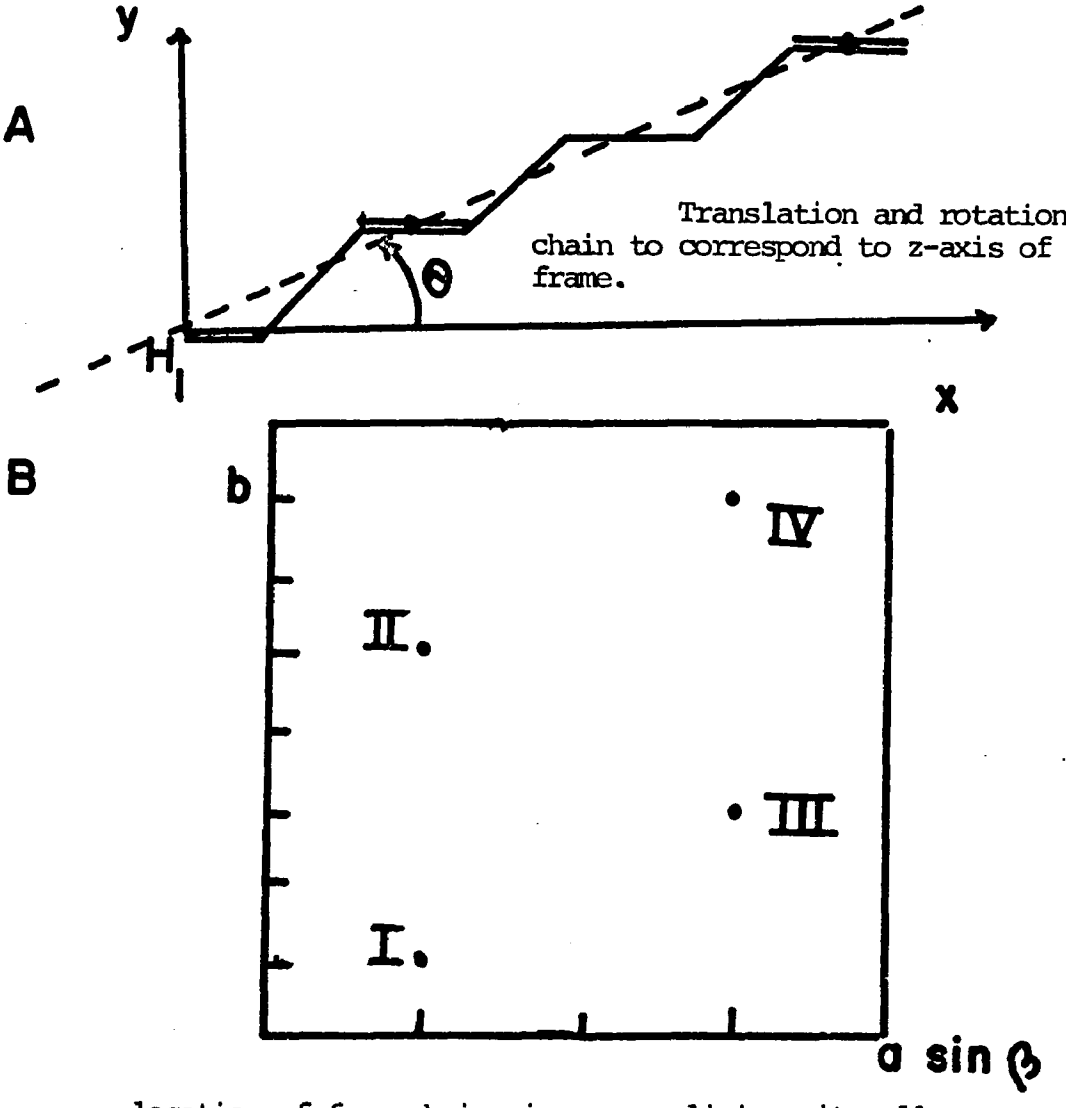
A
y
x
θ
H
Translation and rotation of PTBD chain to correspond to z-axis of laboratory frame.
B
b
IV
II
III
I
a sin β
location of four chains in a monoclinic unit cell
C
II
IV
60°
I
III
INTERCHAIN DISTANCE
location of four chains in an hexagonal lattice

FIGURE 18

3. Obtaining chain III from the coordinates of reoriented chain I by inverting chain I:

all $x' = -x$

all $y' = y$ = unchanged

all $z' = -z$

4. Generating the other two chains:

copy chain I into chain IV

copy chain III into chain II

5. Positioning chains in unit cell or lattice using the following translations:

a. the unit cell: a, b are the lattice constants, β is the monoclinic cell angle. Referring to Figure 18b, the following translations are performed.

	x-translations	y-translations
Chain I	$x' = x + (a \sin \beta)/4$	$y' = y + b/8$
Chain II	$x' = x + (3a \sin\beta)/4$	$y' = y + (b/8+b/2) = y+5b/8$
Chain III	$x' = x + (3a \sin\beta)/4$	$y' = y + 3b/8$
Chain IV	$x' = x + (3a \sin\beta)/4$	$y' = y + (3b/8+b/2) = y+7b/8$

b. the hexagonal lattice: A is the interchain distance. Referring to Figure 18c, the following transformations are performed to create the hexagonal lattice:

	x	y
Chain I	unchanged	unchanged
Chain II	$x' = x + A$	unchanged
Chain III	$x' = x + A/2$	$y' = y + A \sin 60^{o}$
Chain IV	$x' = x + 1.5A$	$y' = y + A \sin 60^{o}$

Generation of a lattice of unit cells

Each cell or chain is then duplicated until a central unit cell is surrounded by 124 other unit cells. These algorithms were tested by creating single chains, unit cells and lattices on the computer and plotting the resulting coordinates, using the same axes as Iwayanagi, et al[31] in their crystallographic study. Plots of a single PTBD chain in the high and low temperature form, from two different perspectives, appear in Figures 19a-c.

Computer experiments on generated chains, cells and lattices

The first set of experiments performed were energy calculations of a single chain as a function of the dihedral angle between two monomer units. Chain lengths of 5, 10 and 20 monomer units were used. Two different energy functions were used, a 6-exp function and a 6-12 Lennard-Jones function (equation 14) with

$$V(r) = -A/r^6 + C/r^{12} \qquad (14)$$

parameters obtained from Scott and Scheraga[58] (SS function) and Kitaigorodsky[67] (K function), respectively. In equation 14, A is given by equation 15, and C is a constant which minimizes the energy at r=R, the sum of the Van der Waals radii. The origin of the parameters used is described below. A complete review of the rationale for selection of non-bonded potential parameters has been given by Ramachandran and Sasisekharan[68].

The net non-bonded interaction between two atoms has most often been represented as the sum of an attractive force plus a repulsive force. Although computational convenience is the main reason for using this two-term idealization of an extremely compli-

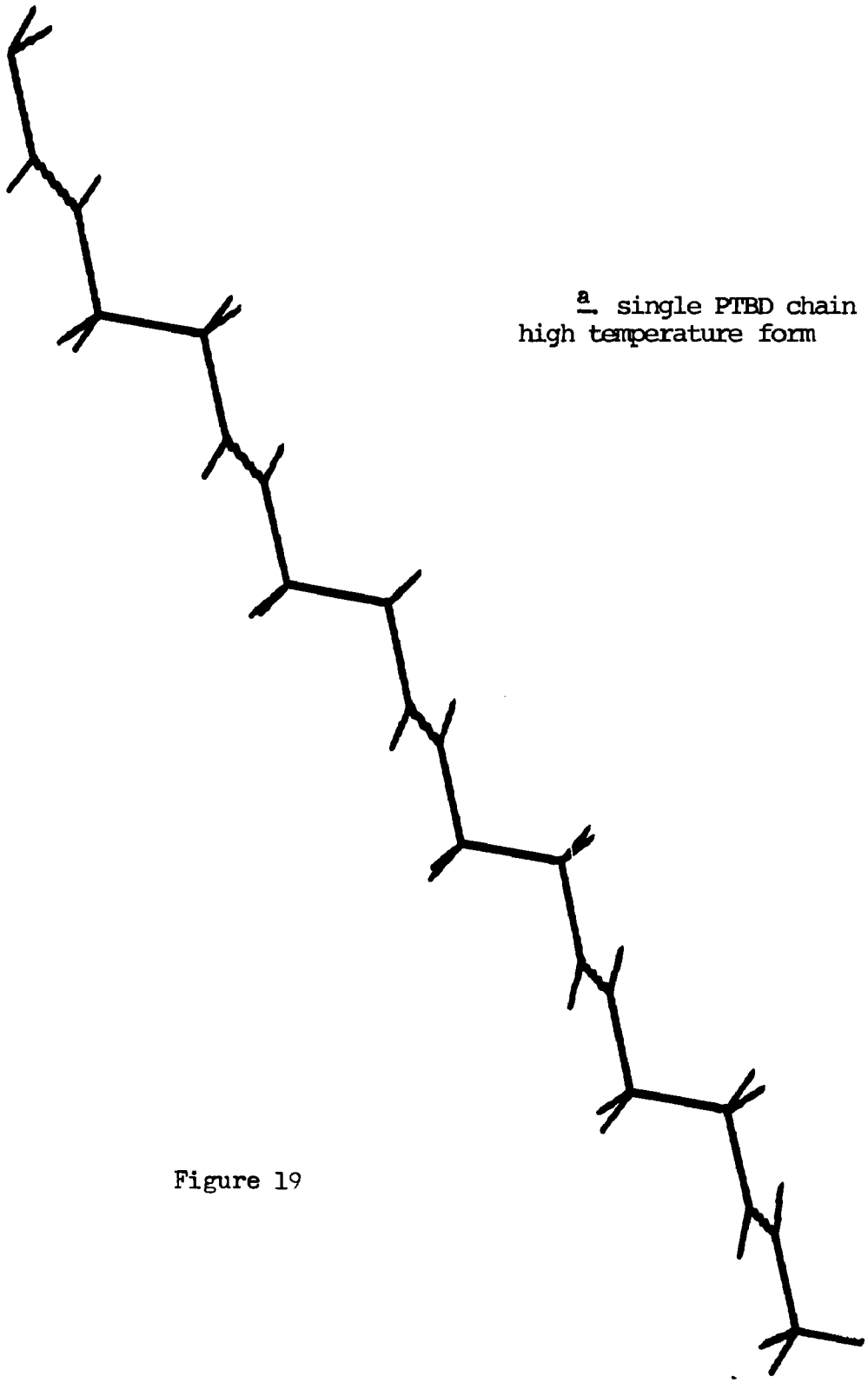

a. single PTBD chain in the high temperature form

Figure 19

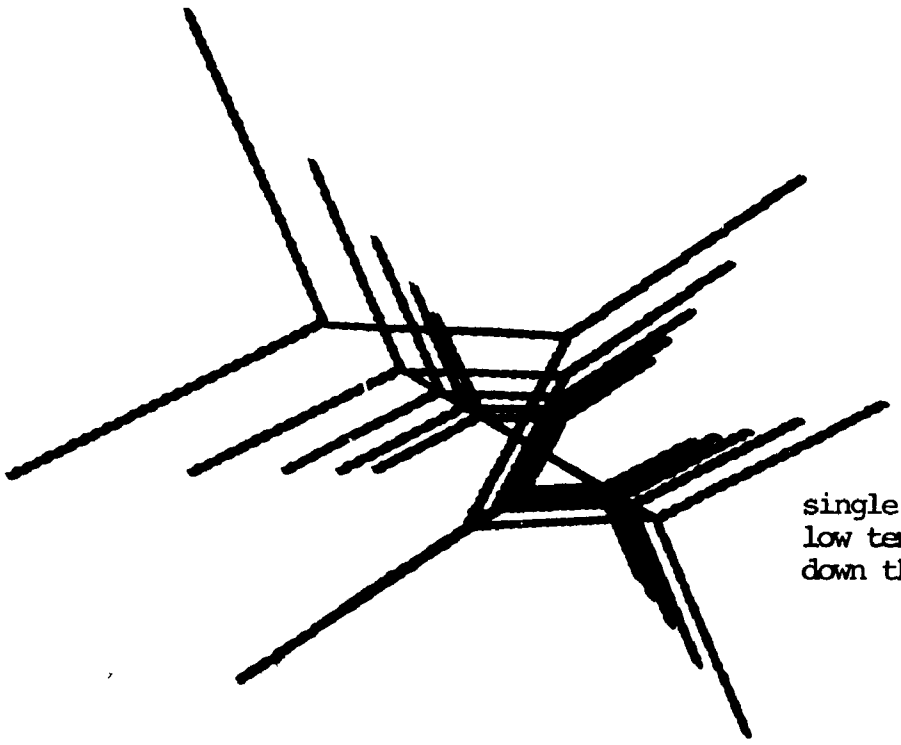

b

single PTBD chain in the low temperature form, looking down the c-axis.

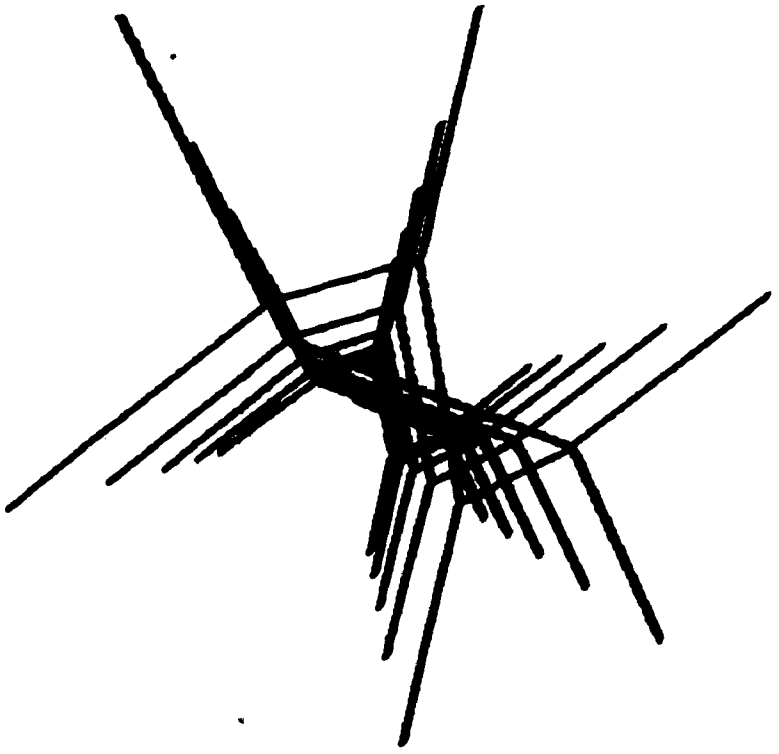

c

single PTBD chain in the high temperature form, looking along the c-axis

Figure 19

cated physical interaction, a weak analogy with well-known interatomic forces serves as the basis for choosing the parameters. The attractive term is taken to be a "Van der Waals attraction" or "London dispersion force", arising from the transient dipole moments created by oscillation of nuclei and electrons within the atoms. The energy of interaction of these dipoles is:

$$V_a = -A/r^6 \qquad (14)$$

where

$$A = \frac{3/2\ e\ (\hbar/\sqrt{m})\ \alpha_1\ \alpha_2}{(\alpha_1/N_1)^{1/2} + (\alpha_2/N_2)^{1/2}} \qquad (15)$$

In equation 15, α_1 and α_2 are the atomic polarizabilities of the two interacting atoms, N_1 and N_2 are the effective number of polarizable electrons on each, and e, m, and $\hbar$ are the usual fundamental constants. Values of these constants are presented in the review of Ramachandran and Sasisekharan.

The repulsive force is ordinarily taken as either

$$V_r = B \exp(-\mu r) \qquad (16)$$

or

$$V_r = C/r^{12} \qquad (17)$$

The steepness and short range of the repulsion are such that either form is adequate within computational limits. This fact was adequately demonstrated by comparing results using the K function versus the SS function, shown below. The constant C in equation 17 is that number which minimizes $(V_a + V_r)$ at r=R, where R is the sum of the van der Waals radii of the two atoms in question.

The parameters used in Equation 18 are not the usual 6-exp ones (Ramachandran, page 363) but are taken from Kitaigorodsky's "universal function", upon the recommendation of Sasisekharan.*

* personal communication to S.D. Stellman

This form of the 6-exp potential was developed specifically for lattice minimizations such as those performed here. Kitaigorodsky's equation is:

$$V_a + V_r = 3.5\ (8600 \exp(-13z) - 0.04z^{-6}) \qquad (18)$$

where z=r/R.

Calculations were made using these two functions (equations 14 and 18) with and without the addition of a threefold sinusoidal torsional terms, given in equation 19.

$$U_{tors} = \frac{V_o}{2} \sum_i (1+ \cos 3\omega_i), \text{ where } V_o=2.00 \text{ kcal/mole.} \qquad (19)$$

The next set of calculations was of the energy of a unit cell and lattice of unit cells. Using the lattice dimensions experimentally derived, an energy was calculated using the Scott and Scheraga (SS) function, equation 20, with the constants shown.

$$\Delta E = \sum_{i<j} a_{cc} r_{ij}^{-6} + \sum_{i<j} b_{CC} r_{ij}^{-12} + \sum_{i<j} a_{CH} r_{ij}^{-6} + \sum_{i<j} b_{CH} r_{ij}^{-12} + \sum_{i<j} a_{HH} r_{ij}^{-6} + \sum_{i<j} b_{HH} r_{ij}^{-12} \qquad (20)$$

where

a_{cc} = -3.70 kcal/mole $\mathring{A}^6$

b_{cc} = 2.80 x 10^5 kcal/mole $\mathring{A}^{12}$

a_{CH} = -1.28 kcal/mole $\mathring{A}^6$

b_{CH} = 38000 kcal/mole $\mathring{A}^{12}$

a_{HH} = -46.7 kcal/mole $\mathring{A}^6$

b_{HH} = 44.60 kcal/mole $\mathring{A}^{12}$

The calculations were carried out on a lattice of 243 cells and a lattice of 125 cells. The energies were found to be very close, indicating that interactions beyond three nearest neighbors did not appreciably affect the energy. All further calculations were carried out on a lattice of 125 unit cells.

The high temperature and low temperature forms of PTBD differ in the c-spacing or dihedral angle defining the plane between monomer units. The low temperature form has a dihedral angle of 109^{o} and the high temperature form an angle of 80^{o}, which shortens the c-spacing of the lattice. Two sets of calculations were carried out using the SS energy function, as well as the Kitaigorodsky (K) energy function. First a fixed dihedral angle of 109^{o} was used and the a and b lattice constants were varied until an energy minimum was found. The lattice constants at the energy minimum were then compared to the lattice spacings found experimentally. The calculation was then repeated using a dihedral angle of 80^{o} for both the K function and the SS function, until new minima were found. The lattice spacings of the high temperature form have not been reported as yet, so that no comparison with experimental data could be made. Both the energy of the unit cell and the lattice were calculated in this way, and the location of minima for the single chain, unit cell and lattice structure were also compared. No torsional term was added into the calculation because torsional terms are a function of the dihedral angle (see equation 19), which in these calculations, remained constant. Thus torsional contributions would simply add a constant term.

The energy calculations were repeated on a hexagonal lattice using the K function. The interchain distance of the lattice was varied and minima for the high and low temperature forms were located. Using the experimentally determined temperature dependence of the interchain distance, the energy was converted from a function of distance to a function of temperature and plotted. Finally, the theoretical heat capacity was found by taking the numerical derivative of the energy curve. The resulting C_p versus temperature curve, as well as the energy versus temperature curve, was analyzed by a standard linear regression analysis and the experimental and theoretical curves compared.

RESULTS

Single Chain Calculations

The effect of chain length on intramolecular energy calculations is shown in Figure 20. The energy was calculated using a 6-exp function, including the torsional term (equation 6). The results indicate that a 20 monomer unit chain length is sufficient to overcome end effects on the chain energy. Lengths of 20 monomer units were used throughout these calculations.

The results of the energy calculations of a single PTBD chain as a function of dihedral angle appear in Figure 21. The graph shows that both the Scott and Scheraga (SS) function and the Kitaigorodsky (K) function without the torsional term predict that the chain has a poorly defined minimum energy at a dihedral angle of 60° but that all angles above 60° are energetically easily accessible to the chain. When the torsional term is added, the energy curves then take on a sinusoidal character and energy minima and maxima are clearly defined. The SS and K functions predict minima at 60° and maxima at 120°.

Single chain calculations predict that the 109° dihedral angle experimentally found for the low temperature form is an energetically unfavorable angle. The single chain calculations also predict that the high-temperature form with the 80° dihedral angle is more stable than the low-temperature form. The energy of a single chain at 109° and 80° for the two functions appears in Table IX.

FIGURE 20

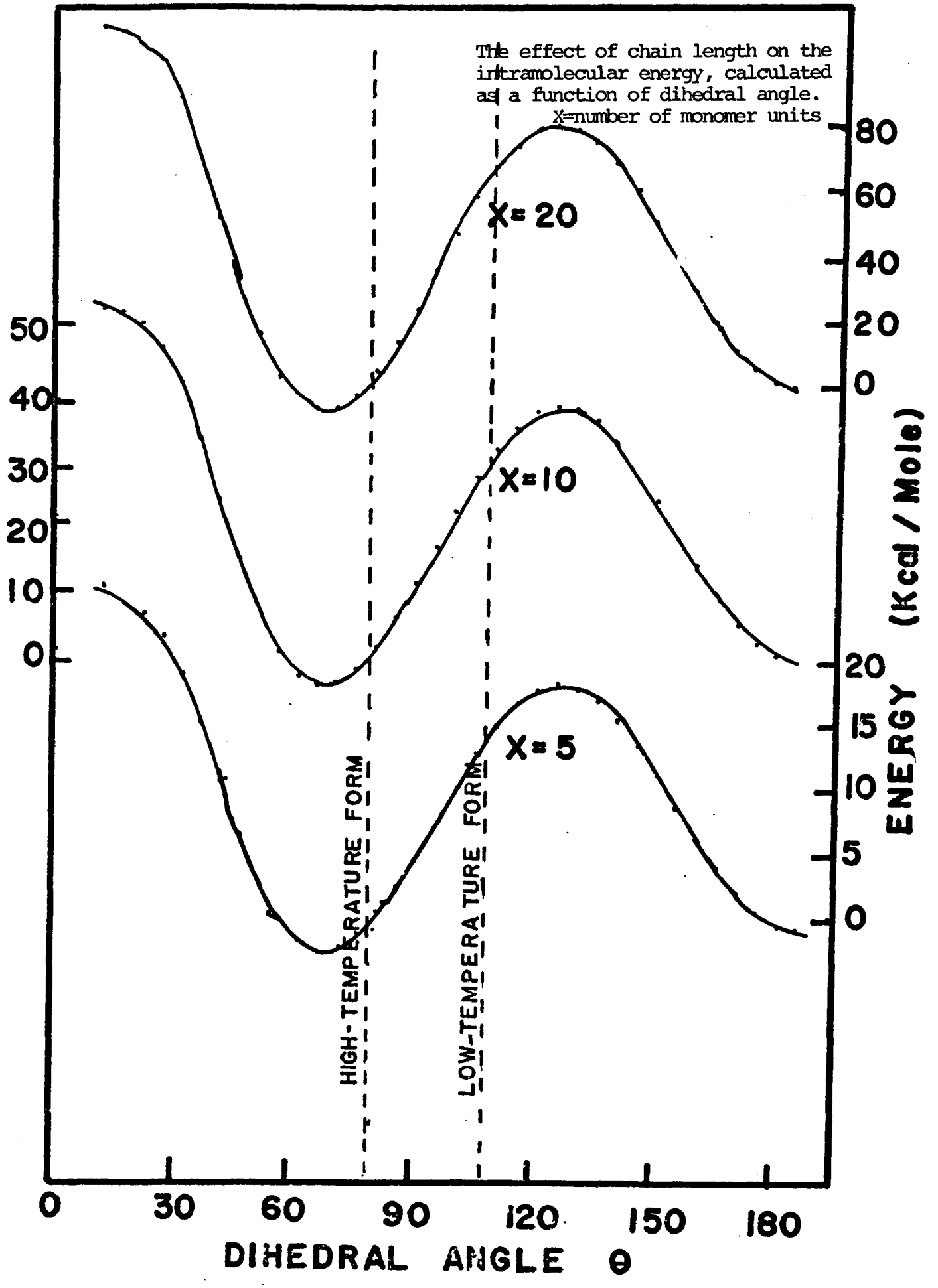
The effect of chain length on the intramolecular energy, calculated as a function of dihedral angle.
X=number of monomer units
X=20
X=10
X=5
HIGH-TEMPERATURE FORM
LOW-TEMPERATURE FORM
ENERGY (Kcal / Mole)
DIHEDRAL ANGLE θ
0
30
60
90
120
150
180
80
60
40
20
0
50
40
30
20
10
0
20
15
10
5
0

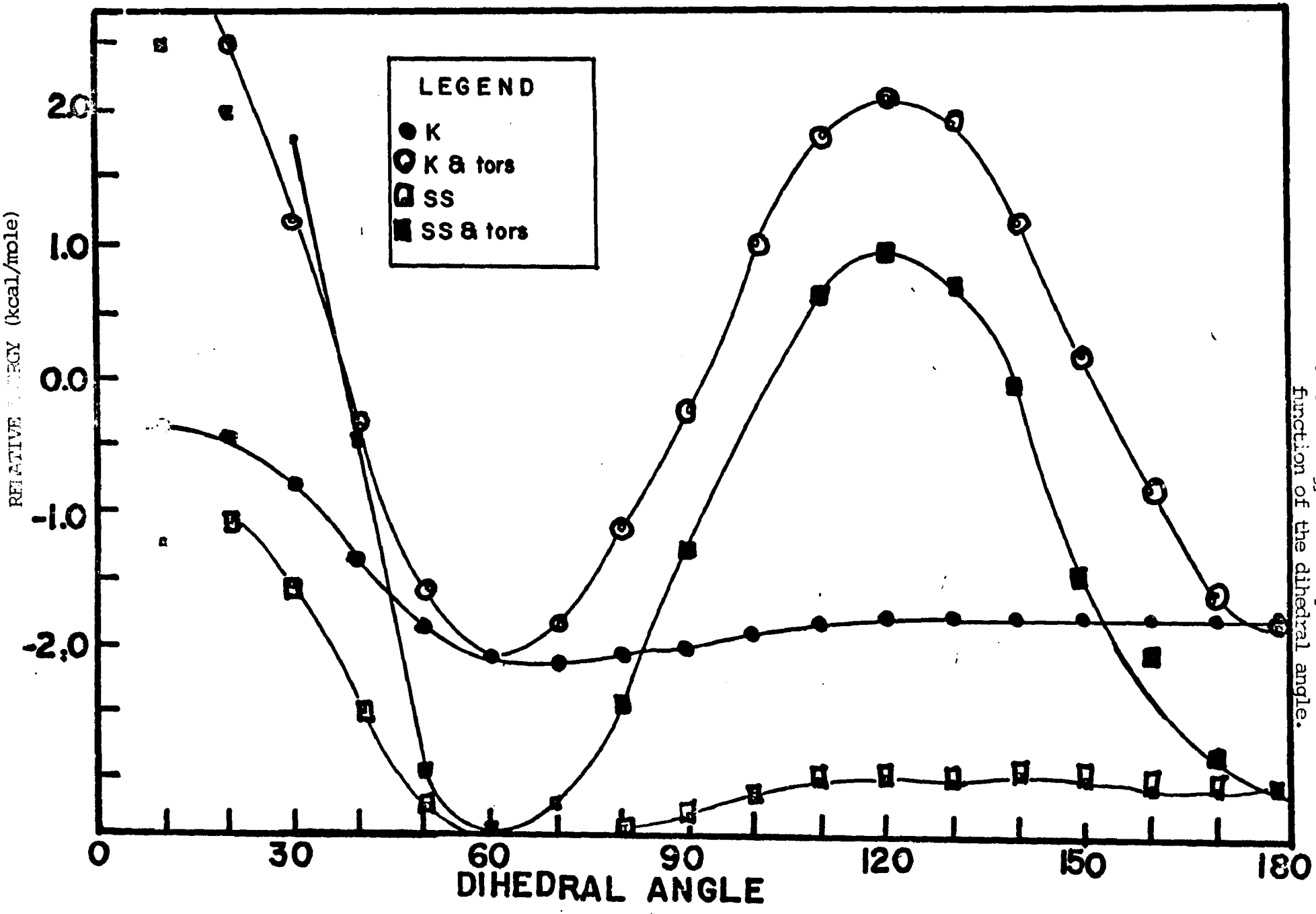

FIGURE 21. The energy of a single PTBD chain as a function of the dihedral angle.

TABLE IX. Calculated Energies of a PTBD Single Chain

Potential Function	Dihedral Angle	Energy (kcal/mole)
SS (no torsional term)	109°	-63.198
	80°	-68.001
K (no torsional term)	109°	-37.726
	80°	-41.781
SS (with torsional term)	109°	-13.454
	80°	-48.001
K (with torsional term)	109°	-36.915
	80°	-21.781

It can be seen that a calculation of the enthalpy of transition would yield a negative result, indicating that the low-temperature form is less stable than the high-temperature form, according to this calculation.

Unit Cell and Lattice Calculations

The location and value of the energy minima for the unit cell and the lattice were found for both the low-temperature and high-temperature forms using the SS and K functions. The results of this minimum energy computer-search appear in Tables X and XI. The Tables consist of that portion of the energy surface that surrounds the minimum energy, which appears with an asterisk. In this calculation , as in the single chain calculations, it is predicted that the high temperature form is energetically more stable than the low-temperature form.

TABLE X . Energy Surface of Monoclinic PTBD Around Minimum Calculated with Scott & Scheraga Function

LOW-TEMPERATURE FORM

b (Å) ↓ \ a → (Å)	8.50	8.55	8.60	8.65	8.70	8.80
9.40			-68.175		-68.293	-67.879
9.50				-69.293	-69.363	-69.091
9.60	-67.544		-69.041		-69.577*	-69.459
9.70			-68.427		-69.201	-69.252

(Energy inkcal/mole)
* Energy minimum

HIGH TEMPERATURE FORM

b (Å) ↓ \ a → (Å)	9.70	9.75	9.80	9.85	9.90	10.00
8.30			-74.896		-74.607	
8.40	-75.508		-75.584	-75.804	-75.649	-75.108
8.50		-75.861	-76.014	-76.017*	-75.904	
8.60			-75.591	-75.654		-75.181

(Energy in kcal/mole)
* Energy minimum

TABLE XI. Energy Surface of Monoclinic PTBD Lattice Around Minimum Calculated with Kitaigorodsky Function

LOW-TEMPERATURE FORM

b (Å) ↓ \ a → (Å)	8.60	8.65	8.70	8.75	8.80
9.45	-40.170	-40.179	-40.158	-40.072	-39.920
9.50	-40.182	-40.212*	-40.209	-40.126	-40.006
9.55	-40.115	-40.184	-40.203	-40.136	-40.020
9.60	-39.982	-40.087	-40.109	-40.070	-39.982
9.65	-39.820	-39.957	-39.985	-39.965	-39.860

(Energy in kcal/mole)
* Energy minimum

HIGH-TEMPERATURE FORM

b (Å) ↓ \ a → (Å)	9.30	9.40	9.50	9.60	9.70	9.80	9.90	10.00
8.10	-37.230		-39.288		-39.487		-38.852	
8.20		-40.188		-41.332		-41.092		-40.323
8.30	-39.468		-42.008		-42.441		-41.952	
8.40		-41.501		-42.959		-42.957		-42.281
8.50	-39.452		-42.559		-43.289*		-42.947	
8.60			-40.964	-42.881		-43.094		-42.524
8.70	-37.886		-41.610		-42.691		-42.530	

(Energy in kcal/mole)
* Energy Minimum

The observed lattice constants of the low-temperature form are given as $\underline{a}$= 8.63Å, $\underline{b}$=9.11Å, $\underline{c}$=4.83Å and β=114°.[31] The coordinates of the calculated energy minima for both energy functions are quite close to the experimental value. The lattice constants found by the SS function deviate 0.07Å for the $\underline{a}$ constant and 0.49Å for the $\underline{b}$ constant. The deviation of the $\underline{a}$ constant is 0.07Å and the $\underline{b}$ constant is 0.37Å for the minimum energy found with the K function. No lattice constants are available for the high-temperature form.

Calculations of the energy of an hexagonal lattice as a function of interchain distance were also performed using the K function. The results of these calculations appear in Figures 22 and 23. It can be seen that there is a clearly defined minimum at 4.60Å and 4.67Å for the low temperature and high temperature forms, respectively.

Although the structural studies of the high temperature form did not define a space group or yield lattice constants, Suehiro and Takayanagi have found[32] that in the high temperature form each molecular chain is hexagonally surrounded by six other chains which are equidistant from each other. At room temperature the interchain distance observed is 4.60Å, and the minimum interchain distance for the high temperature form is 4.95Å. A plot of the interchain distance versus temperature data appears in Figure 24.

It is seen that the K function accurately predicts the lattice constants at the energy minimum for the low temperature

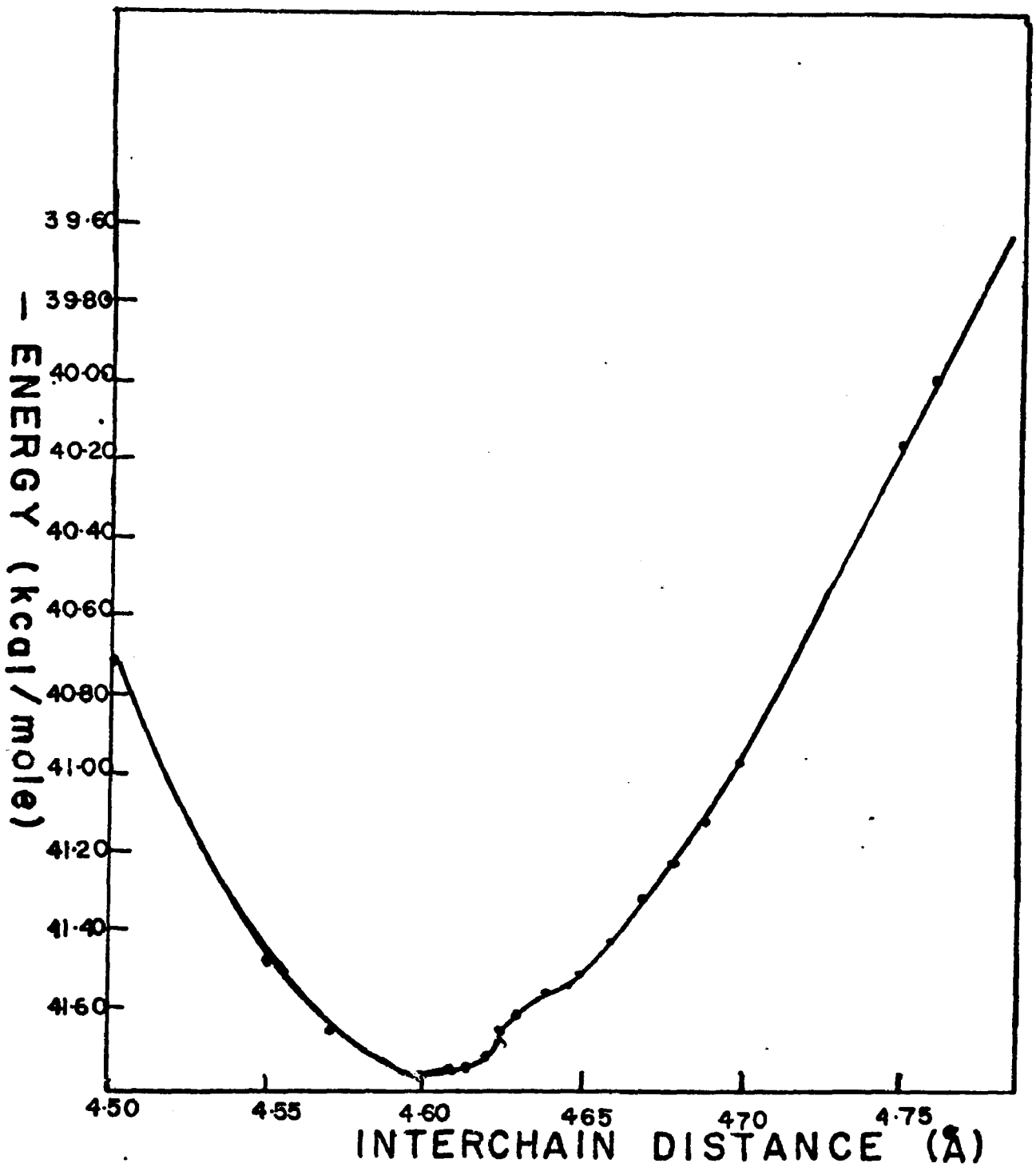

FIGURE 22
Energy of an hexagonal low-temperature PTBD lattice as a function of interchain distance, calculated using the Kitaigorodsky potential function.

FIGURE 23. Energy of an hexagonal high-temperature PTBD lattice as a function of interchain distance, calculated using the Kitaigorodsky potential function.

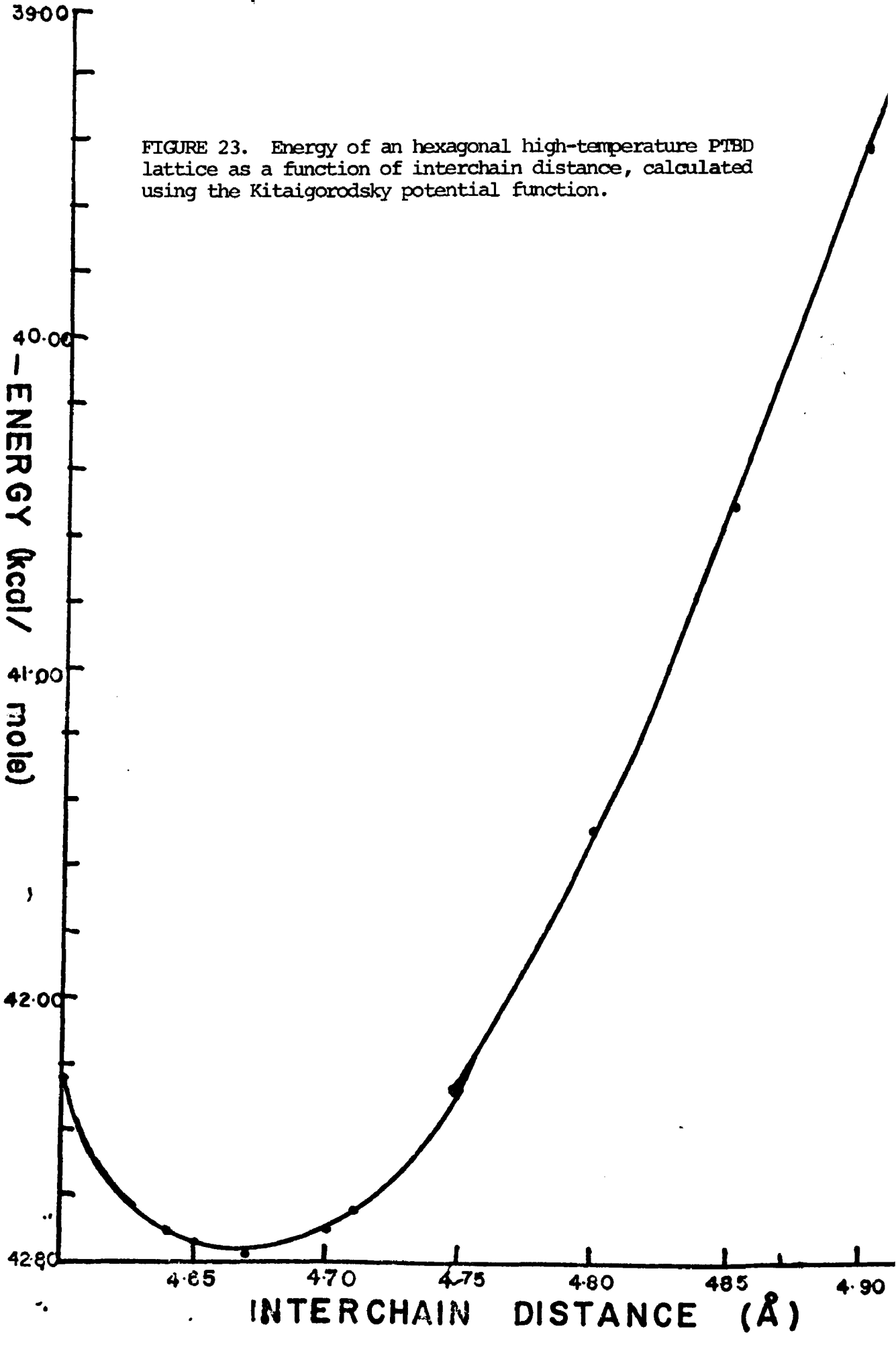

FIGURE 23

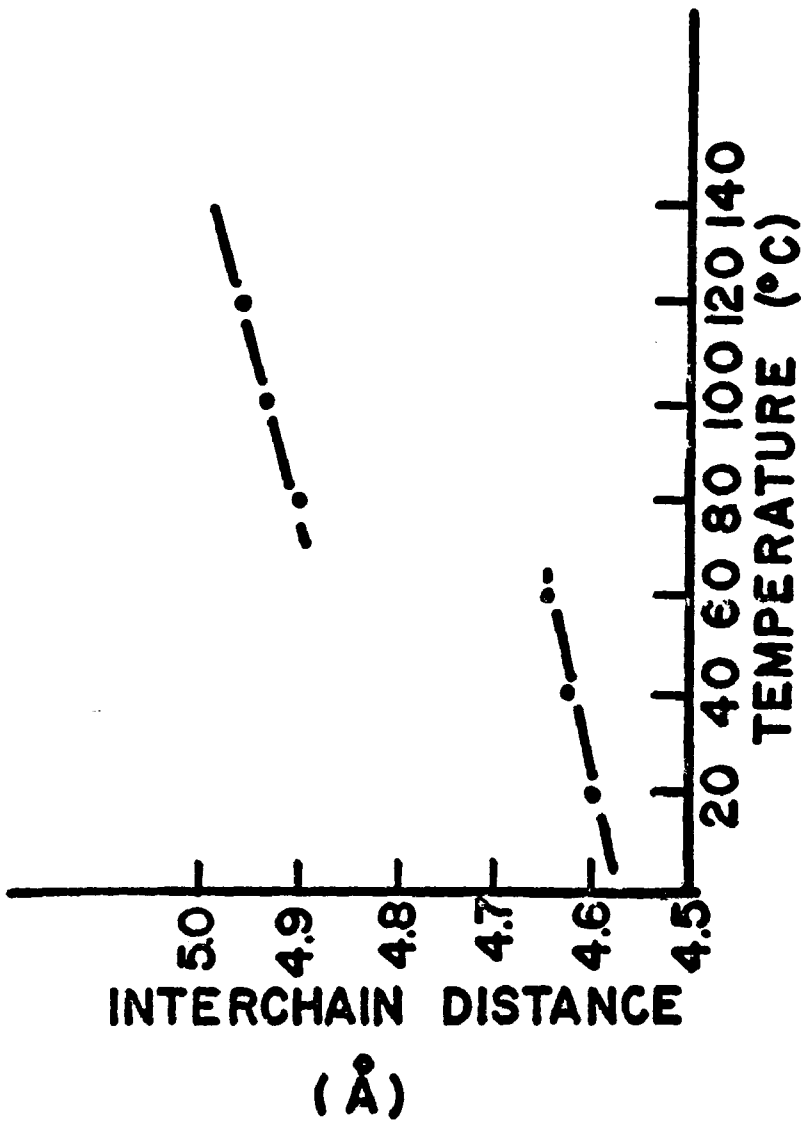

FIGURE 24

Experimental interchain distance as a function of temperature, taken from reference 32.

form, but predicts constants for the high-temperature form which are far too small in comparison with the experimental values.

It is interesting to compare the location and value of the energy minima found for the monoclinic and hexagonal lattices with those found for the unit cell. These comparisons are summarized in Table XII. In each case the value of the energy of the lattice represents a structure that is well over six times as stable as the structure corresponding to the minimum value calculated for the unit cell. When the energy of the unit cell is compared with the energy calculated for four single chains, it is seen that the unit cell is in turn far more stable than the sum of the energies of the four chains. These results appear in Table XIII.

In the hexagonal lattice calculation (Table XII) the minimum energy of the single chain occurs at an interchain distance of 4.94Å while the minimum of the lattice is at 4.67Å. Thus, unlike the lattice, the coordinates of the minimum for the unit cell are very close to the experimentally observed interchain distance.[32] The heat of transition calculated from the hexagonal lattice data given in Table XII is in reasonable agreement with experiment. The difference between the energy minimum of the low temperature form and the energy of the lattice at 4.90 Å, the experimental interchain distance, is equal to 43.5 cal/gram. If one uses the energy of the lattice at the coordinates of the calculated energy minimum for the unit cell (4.97Å), the heat of transition is found to be 59.8 cal/gram. The heat of

TABLE XII. Comparison of the value and location of the energy minima

a. monoclinic lattice and the unit cell

Potential Function	Temperature Form	Lattice Energy (kcal/mole)	Energy of Unit Cell (kcal/mole)	Lattice Spacings a (Å)	b (Å)
SS	low temp.	-69.577*	-11.146	8.70	9.60
		-67.544	-11.592*	8.50	9.60
SS	high temp.	-76.017*	-12.146	9.85	8.50
		-75.654	-12.362*	9.85	8.60
K	low temp.	-40.212*	- 6.942	8.65	9.50
		-39.449	- 7.247*	8.45	9.50
K	high temp.	-43.289*	- 7.548	9.70	8.50
		-29.33	- 8.625	9.10	8.70

b. hexagonal lattice and the unit cell

				interchain distance (Å)
K	low temp.	-41.761*	- 7.090	4.60
		-41.559	- 7.111*	4.64
K	high temp.	-42.788*	- 4.192	4.67
		-38.531	- 6.273*	4.94
K	high temp.	-39.411	- 6.225	4.90 †

* Energy minima

† The experimental data indicate that the high temperature form does not exist below an interchain distance of 4.90 Å. Thus only the local minimum, not the absolute minimum makes sense experimentally.

TABLE XIII. Calculated Energies of a Unit Cell and Four Single Chains

Function	Minimum Energy Unit Cell (cal/g)	Energy of Four Chains (cal/g)
Low-temperature		
SS	- 11.592	-4.618
K	- 7.247	-2.602
High-temperature		
SS	- 12.363	-5.041
K	- 8.625	-2.887

transition found experimentally for heptane grown melt-recrystallized sample is 27 cal/gram (see Table V).

Comparison of Experimental and Theoretical Heat Capacity

By using the interchain distance versus temperature data of Suehiro and Takayanagi[32] (see Figure 24) and the calculated energy versus interchain distance data shown in Figures 22 and 23, the energy as a function of temperature was derived. This data is plotted in Figure 25. The energy for the high temperature form was found to be a linear function of temperature. A linear regression analysis showed a regression coefficient of 0.998. It can be seen that the energy for the low temperature form is not a linear function of temperature.

Using this energy versus temperature data in conjunction with the experimental data for the heat capacity and energy presented in Figures 15 and 16, respectively, the following comparisons were made. Choosing four arbitrary temperature ranges, the experimental and theoretical energies were plotted as a function of temperature. Figure 26 shows the values of the ΔH for each range. The heat capacity, C_v, is equal to the derivative of an energy versus temperature curve. It can be seen that for each of these ranges the experimental slope, or derivative curve, is always greater than the slope of the theoretical curve.

For the linear high temperature form a numerical difference for the entire range can be calculated. The slope of the calculated energy versus temperature curve for the high temperature form was 0.13 cal/gram-°C. This value was compared to the experi-

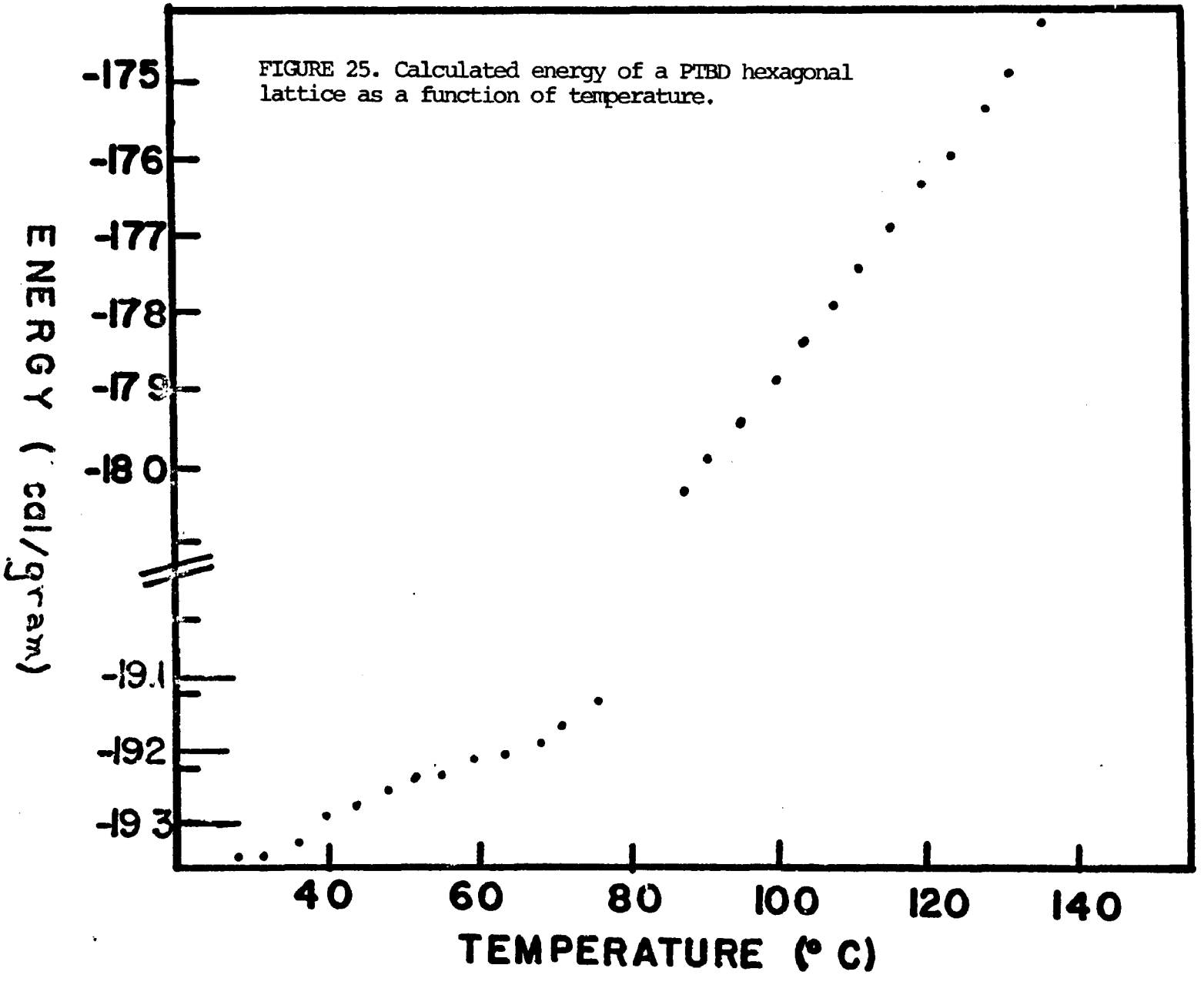

FIGURE 25. Calculated energy of a PTBD hexagonal lattice as a function of temperature.

FIGURE 25

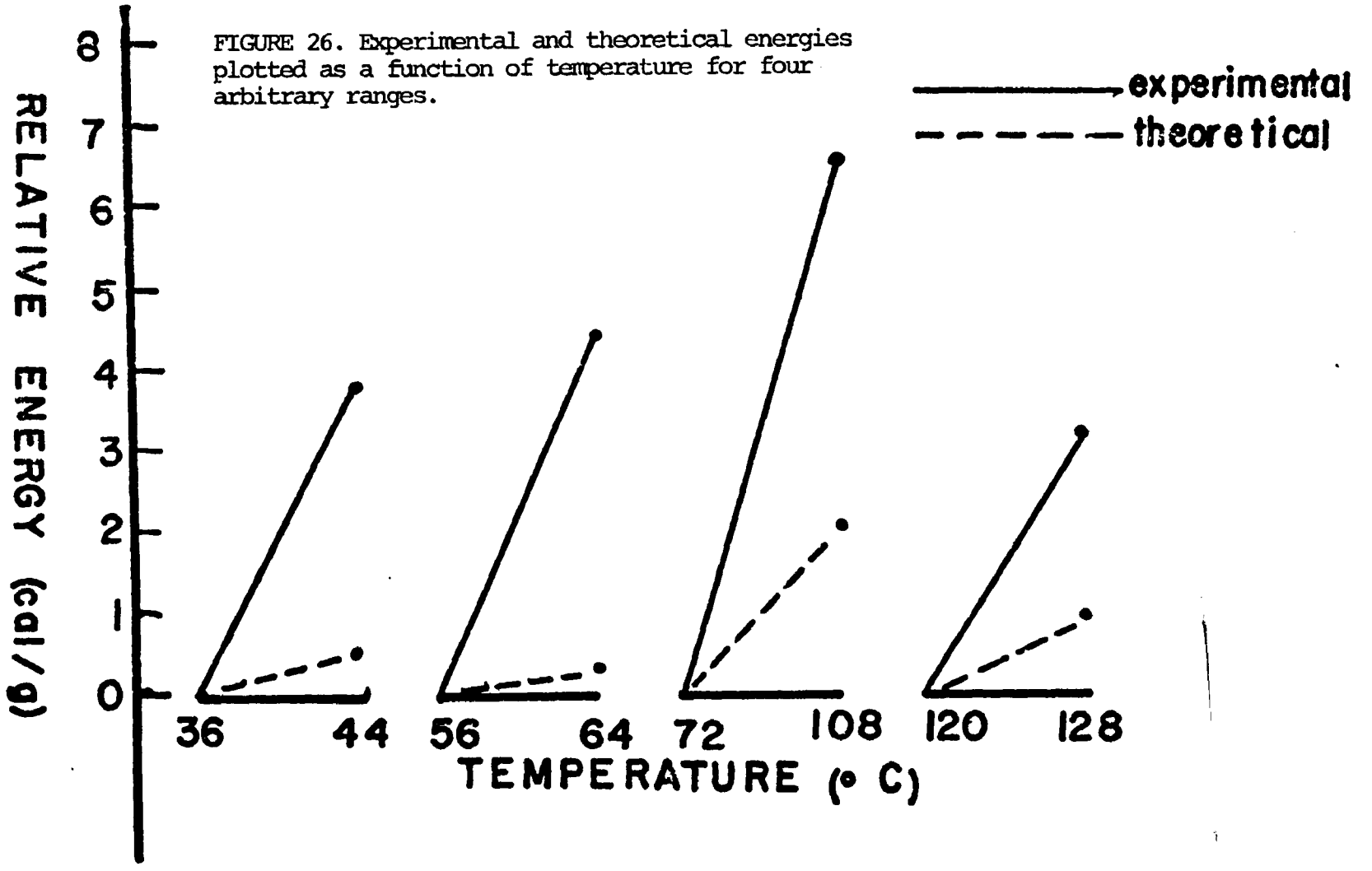

FIGURE 26. Experimental and theoretical energies plotted as a function of temperature for four arbitrary ranges.

FIGURE 26

mentally obtained heat capacity. It was found that the difference between these two values was 0.28 cal/gram-°C.

DISCUSSION

The purpose of these calculations has been twofold. One aim has been to test many of the assumptions and theories that are commonly encountered in the literature in this type of study. As was discussed previously, PTBD lends itself very well to this purpose because it undergoes a solid-solid phase transition. The second aim of this study has been to further elucidate the observed physical properties of PTBD. Since at the present state-of-the-art, all theoretical results must be appreciated in terms of their limitations, the order of discussion will first be to discuss the limits of the theoretical approach and then, with these limits in mind, to discuss the implications of the calculational results on our understanding of the structure of PTBD.

Single Chain Calculations

Figure 21 is a plot of the energy of a single PTBD chain as a function of the dihedral angle. Because the monomer unit is planar, containing a double bond which hinders other rotation, the conformation of the entire chain is determined by the dihedral or settle angle, θ . Thus once the other bond angles and distances are set, θ is the only parameter used in an energy calculation for a helical chain like PTBD. Inspection of Figure 21 shows that it is essential to add in a torsional term to the potential function in order to predict any real selectivity in chain orientation.

Without the torsional term there is a small energy well

at 60° and then all dihedral angles are practically equipotential, so that no preferred conformation above an angle of 60° is predicted. Once the torsional term is added, a sinusoidal character is imposed upon the potential diagram. However, the conformation that is predicted to be the most stable occurs at a dihedral angle of 60? As noted previously, the high temperature form is more stable than the low temperature form, according to this calculation.

Inspection of the plots also reveals that the two potential functions yield energy diagrams with the same overall character. The only difference between the results is one of relative energies. However, since experimentally derived energies are really energy differences, the fact that the two functions predict different values for the energy is not significant.

Thus the conclusion that can be drawn is that single chain calculations are apparently insensitive to the potential function used. They also appear to be wholly unsatisfactory without the addition of torsional terms. In addition, when the torsional terms are included, the conformations that are predicted to be the most stable are not the conformations found experimentally, and therefore, are not the true energy minima.

A discussion of the ramifications of these conclusions on commonly accepted theories and practices will be deferred until the lattice and unit cell have been discussed.

Unit Cell and Lattice Calculations

In assessing the success of a theoretical calculation such as the minimization of the energy for the two forms of PTBD, we

seek comparison with available experimental data. In this case, it would seem obvious to compare the theoretical heat of transition with the experimentally observed enthalpy of transition. As in the case of the single chain calculation, a calculation of the energy difference for the hexagonal lattice, the unit cell or four hexagonally oriented chains, all yield a negative heat of transition. This, of course, indicates that according to these calculations, the polymer is more stable with the lattice constants predicted for the high temperature form than at the coordinates that minimize the energy of the low temperature form. This result is found for calculations done with both the K and SS functions (see Tables X, XI and XII).

At this point the results seem to show that the calculations are not realistic. However, if one looks at the predicted coordinates rather than just at the energy difference, several points of interest become apparent. As discussed in the previous section, although the structure of PTBD in the high temperature form has not been assigned to a specific space group, data on the interchain distance in an hexagonal array is available[32] (see Figure 24). The minimum interchain distance found in the high temperature form is 4.90 Å. The calculations locate the minimum energy of the high temperature form at 4.67Å (see Figure 23), an experimentally determined unrealizable configuration for the crystal. The predicted interchain distance for the low temperature form was 4.60Å, in exact agreement with the experimentally observed value.

The significance of this observation is far-reaching.

The very basis of this type of theoretical approach is the concept that the conformation of the macromolecule at the minimum potential energy is also the conformation of the macromolecule at the minimum free energy.[56-68] But free energy, ΔG, has two thermodynamic components, the enthalpy, ΔH, and the entropy, $T\Delta S$. Minimizing the potential energy only deals with the minimization of the enthalpic contribution to the free energy and totally ignores the entropic contribution.

With this in mind, one must examine the observed experimental calorimetric and heat capacity results discussed in Part I. There the conclusion drawn was that the chains in the high temperature form contain a great deal of torsional freedom, and, in fact, that in essence, all realizable conformations were accessible to the crystal. The calorimetric measurements for the crystals concurred with those previously observed for the bulk polymer[45], and showed that the entropy of transition from the low temperature form to the high temperature form was almost twice the entropy of melting. Thus the entropic contribution to the free energy of the crystals is quite significant.

The agreement obtained between experimental and calculated values for the coordinates of the low temperature form is excellent, however. Both the K and SS functions in the monoclinic lattice arrangement, as well as the K function in the hexagonal array, predict the experimentally observed configuration well. An inspection of the model of the low temperature form shows that there is little room for torsional motion in the lattice. The rising heat capacity as a function of increasing temperature

that is observed experimentally indicates that there is a rapid rise in the number of conformations accessible to the chains. According to the x-ray studies[32] this is accompanied by a linear increase in the interchain distance within the lattice. Thus at the lower temperatures, the enthalpic contribution to the free energy is the major one, and minimization of the potential energy is approximately equivalent to the minimization of the free energy.

A comparison of the values for the energy of the unit cell and lattice of 125 unit cells (Table XII) shows that there is a stabilizing effect of the lattice structure. This stabilization is also observed for the unit cell which has an energy less than is calculated for four single chains (Table XIII). Thus the conclusion previously drawn that single chain intramolecular energy calculations cannot be used to estimate the energy of a crystalline solid is further verified. In fact, for such solids, it becomes apparent that even the energy calculated for a unit cell is not an adequate measure of the energy of a lattice.

Implications for Many Existing Models

The implications of these results on the majority of theoretical polymer calculations are far-reaching. The validity of the use of Flory[51] and Volkenshtein[56] calculational methods for polymeric solids is called into question. In essence, as discussed previously, this method concerns itself with assigning statistical weights to the various rotational isomers of a single chain. When possible these statistical weights are arrived at from experimental determination of the rotational barriers of

small molecules. From the statistical weights, the partition function can be calculated, and hence all the thermodynamic properties.

Using this method Mark[49,50] calculated many of the solution properties of PTBD. Flory and Abe[52] carried out a study of the conformational interactions of -1,4- butadiene structural units ($-CH_2-CH_2-CH_2-CH=$) and their effect on the properties of polybutadiene. They also calculated solution properties. A result obtained was that introduction of stereoirregularity into a single chain had a greater effect on predominantly trans chains than on predominantly cis chains.

In light of the results obtained here, questions can be raised as to the real meaning of a study such as the Flory and Abe investigation. It has been shown here that the contribution of the intramolecular interactions of a single chain are not equivalent to all the interactions occurring in a solid. Apparently, the interactions that determine the minimum energy configurations and conformations in a real system are not predominantly intramolecular. Hence, intramolecular energy calculations are, in essence, a mathematical study of the minima of the particular function used, and not a study of a polymeric system. In his work on PTBD, Mark[49,50] concluded that a calculation of the energy of a PTBD lattice was necessary to evaluate the validity of his method. The calculations performed here verify his conclusion that such a study was necessary. The results of these calculations indicate that single chain configurational statistics are invalid models for real solid systems.

Corradini, et al[71] have applied the Flory method to

chain folding in PE single crystals in an effort to see the cooperative effect of bond angle deformation and rotational strain. They minimize the energy of a single PE chain bent into various geometries and conclude that the fold energy appears to be essentially due to the sum of the torsional and bending contributions. Again, in light of the data presented here, before the conclusions of Corradini, et al, can be drawn, it is essential to construct a surface consisting of many chains and then to minimize the energy of this surface, in order to evaluate the contribution of the lattice stabilization energy to the minimum free energy conformations. Only then would it be possible to assess the accuracy of single chain statistics in predicting the surface structure of PE crystals.

In addition, given the fact that the surface is not perfectly crystalline, the evaluation of the entropic contribution to the free energy is also necessary. This is a more difficult problem, probably involving a numerical evaluation of the partition function.

The PTBD Model --- The Lattice Structure

The fact that the K function accurately predicts the interchain distance of the low temperature form indicates that it is a good energy function for the system and that models for PTBD can be inferred from these calculations with reasonable confidence. Using the K function, minimum energies for a monoclinic and an hexagonal lattice (see Table XII), it is found that the difference in energy between these two structures is

1.549 kcal/mole for the low temperature form and 0.501 kcal/mole for the high temperature form. In the case of the high temperature form, the difference in energy is less than kT, indicating that both forms are energetically accessible to the crystal. In actuality, the energy difference should be taken between the calculated energy for an interchain distance of 4.90Å for the hexagonal lattice and the energy at the corresponding experimental lattice constants for the monoclinic form. However, since the lattice constants are not known, this cannot be done. Since the behavior of the two functions is quite similar, however, it is reasonable to assume that the energy difference would be about the same for the configurations corresponding to the actual experimental data.

An inspection of the energy surfaces (Table X and XI) reveals that the energy minima for PTBD are quite shallow and rather large changes in lattice dimensions produce small changes in the energy. This becomes more apparent when the PTBD data is compared to typical data found in the literature. In their study of the energies of various tetraphenyl organo-metallic compounds, Ahmed, Kitaigorodsky and Mirskaya[66] calculated the energies of various crystals as a function of internal rotational angles. Their results for tetraphenyl tin appear in Figure 27, a surface contour of the variation of the energy (in kcal/mole) with θ, the angle of rotation of the phenyl groups around the tin bond, and ϕ, the angle of rotation of the molecule about the C_4 (z) axis in the crystal. The 10 kcal/mole change in the contour corresponds to a change of only 0.39Å. Comparison with the PTBD energy surface shows that the tin compound has a much deeper

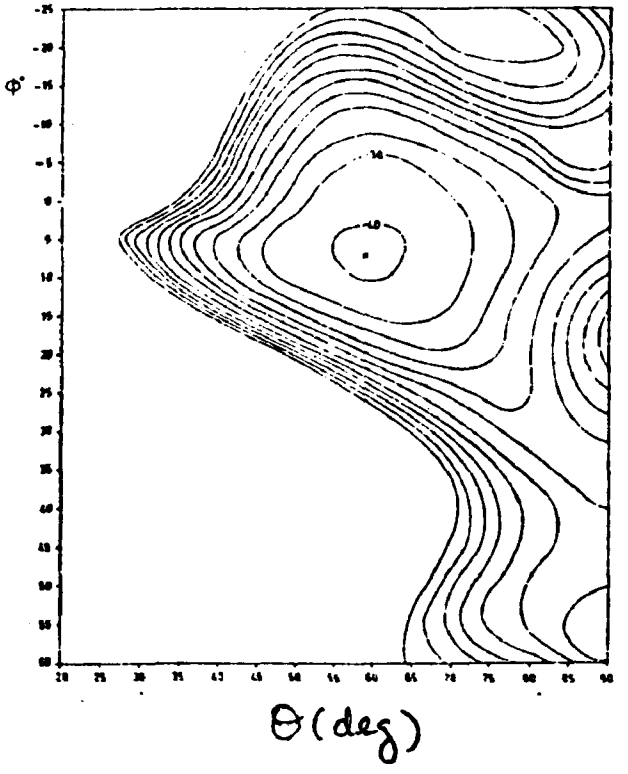

FIGURE 27

Variation of energy of tetraphenyltin as a function of two conformational angles, taken from reference 66.

energy well. This is typical of many molecules.

The shallowness of the energy well indicates that PTBD has considerable freedom of motion, even at the configuration corresponding to the potential minimum, because the energy barriers between configurations are comparatively low. Thus even with an energy difference of about 2kT for the low temperature form, both the hexagonal and monoclinic lattice structure are energetically accessible and much interconversion between these forms and the various configurations between these forms can be expected. This could explain the "pseudo-hexagonal" crystal structure attributed to PTBD in the x-ray investigation.[31] It could also explain the difficulty in obtaining a specific crystallographic space group for the high temperature form.[32] The interconversion between the two forms could be so great as to make it extremely difficult to obtain a clear pattern.

The PTBD Model -- Transition and Lattice Energies

The heat of transition that is predicted for PTBD is 43.5 cal/gram. This value is arrived at by taking the difference between the minimum energy of the low temperature form and the energy at an interchain distance of 4.90Å for the high temperature form (see Table XII). The energy at 4.90Å is used rather than the calculated minimum energy because, as discussed previously, the calculated minimum falls at an experimentally unrealizable distance. It is valid to use the energy at 4.90Å even though it is not a minimum because the interaction between the atoms is about the same at 75°C, the temperature of the high temperature form,

as at room temperature. Thus one would expect that the K function would remain a good function for describing these interactions until electronic transitions begin occurring in the crystal, which, of course, would be at a much higher temperature. The calculated value for the transition is a little less than double the experimental heat of transition for melt recrystallized heptane crystals (see Table IV). This is good agreement and as good as one could expect between the actual solid and a model of a perfect, motionless crystalline lattice.

It is interesting to note that the configuration corresponding to the minimum free energy of the unit cell for the high temperature form occurs at an interchain distance of 4.94Å, quite close to the experimental value. Thus it would seem that lattice stabilization energy is not a determining factor in the minimum free energy configuration of the crystals in the high temperature form.

The difference of 0.28 cal/gram-°C or 60 cal/mole-°C, between theoretical and experimental energy-temperature plots indicates that about two-thirds of the heat capacity of the high temperature form is due to lattice motions. If, as a first approximation, one uses the law of Dulong and Petit for an estimate of the heat capacity due to lattice motions, about 54 cal/mole-°C are left for low-energy vibrations. The Dulong and Petit value of 6 cal/mole-°C is an estimate for monatomic crystals and probably underestimates the energy of the modes of a polymer lattice. However, the approximate value of 54 cal/mole-°C indicates the probability of finding several chain vibrations below 200 cm^{-1} in the far IR.

CONCLUSIONS

Intramolecular energy calculations of single chain interactions alone were found to be an insufficient measure of intermolecular interactions in a real solid. At low temperatures, the lattice stabilization energy is a dominant factor in determining the minimum free energy configuration. Once there are torsional freedom and defects in the solid, the entropy effects can no longer be neglected and therefore, minimization of the potential energy is not equivalent to minimization of the free energy.

In PTBD the energy barriers between the hexagonal lattice and a lattice of monoclinic unit cells were found to be low enough to allow interconversion between these structures. At the larger interchain distances of the high temperature form, lattice stabilization energy was found to have a smaller effect on the minimum free energy configuration. The heat capacity of the high temperature form can be largely attributed to lattice and torsional motions.

REFERENCES

1. A. Keller, Phil. Mag. 2, 1171 (1957).
2. P. H. Geil, "Polymer Single Crystals," Interscience, New York (1963).
3. P. H. Lindenmeyer, Science 147, 1256 (1965).
4. J. D. Hoffman, Soc. Plastic Eng. 4, 315 (1964).
5. P. H. Geil, J. Polymer Sci. 44, 449 (1960).
6. P. H. Geil, J. Polymer Sci. 47, 65 (1960).
7. J. D. Hoffman, J. I. Lauritzen, E. Passaglia, G. S. Ross, L. J. Frolen, and J. J. Weeks, Kolloid-Z. 231, 564 (1969).
8. A. Peterlin and G. Meinel, J. Polymer Sci. B3, 1059 (1965).
9. A. Peterlin, G. Meinel, and H. G. Olf, J. Polymer Sci. B4, 399 (1966).
10. D. J. Blundell, A. Keller, and T. Conner, J. Polymer Sci. A2, 5, 991 (1967).
11. E. W. Fischer and G. Schmidt, Angew. Chem. 74, 551 (1962).
12. P. J. Flory, J. Am. Chem. Soc. 84, 2857 (1962).
13. R. J. Roe and H. E. Bair, Macromolecules 3, 454 (1970).
14. A. Keller, E. Martuscelli, D. J. Priest, and Y. Udagawa, J. Polymer Sci A2, 10, 1807 (1971).
15. R. J. Roe, J. Chem. Phys. 53, 3026 (1970).
16. M. I. Bank and S. Krimm, Bull. Am. Phys. Soc. Ser. II, 14, 442 (1969).
17. S. Krimm and M. I. Bank, Preprints of Papers Presented at International Symposium on Macromolecular Chemistry, IUPAC, Toronto, Canada, Paper 26-18 (1968).
18. J. L. Koenig and M. J. Hannon, J. Macromol. Sci.-Phys. B1, 119 (1967).

19. J. L. Koenig and M. C. Agboatwalla, J. Macromol. Sci.-Phys. B2, 391 (1968).

20. F. H. Winslow, M. Y. Hellman, W. Matreyek, and R. Salovey, J. Polymer Sci. B, 5, 89 (1967).

21. D. J. Blundell, A. Keller, I. M. Ward, and I. J. Grant, J. Polymer Sci. B, 4 781 (1966).

22. T. Williams, D. J. Blundell, A. Keller, and I. M. Ward, J. Polymer Sci. A-2, 6, 1613 (1968).

23. D. M. Sadler, T. Williams, A. Keller, and I. M. Ward, J. Polymer Sci. A-2, 7, 1819 (1969).

24. A. Keller and Y. Udagawa, J. Polymer Sci. A-2, 1793 (1971).

25. D. J. Priest, J. Polymer Sci. A-2, 9, 1777 (1971).

26. A. Keller and D. J. Priest, J. Macromol. Sci. B, 2, 479 (1968).

27. A. Keller and D. J. priest, J. Polymer Sci. B, 8, 13 (1970).

28. S. Krimm and M. I. Bank, J. Polymer Sci. A-2, 7, 1785 (1969).

29. I. M. Kolthoff, T. S. Lee, and M. A. Mairs, J. Polymer Sci. 2, 199 (1947).

30. I. M. Kolthoff and T. S. Lee, J. Polymer Sci. 2, 206 (1947).

31. S. Iwayanagi, I. Sakurai, T. Sakurai, and T. Seto, J. Macromol. Sci.-Phys. B2, 163 (1968).

32. K. Suehiro and M. Takayanagi, J. Macromol. Sci.-Phys. B4, 39 (1970).

33. S. Takamuku, T. Tatsumi, and M. Takayanagi, Reports on Progress in Polymer Physics in Japan, X, 333 (1967).

34. J. F. Jackson and L. Mandelkern, Macromolecules 1, 546 (1968).

35. R. K. Sharma and L. Mandelkern, Macromolecules 3, 758 (1970).

36. R. K. Sharma, J. F. Jackson, and L. Mandelkern, Macromolecules 3, 763 (1970).

37. A. Nakajima, F. Hamoda, S. Hayasaki, and T. Sumida, Kolloid-Z. 222, 10 (1968).

38. T. Kawai and A. Keller, Phil. Mag. 11, 1165 (1965).

39. H. Bair and R. Salovey, Macromolecules 3, 677 (1970).

40. J. F. Jackson and L. Mandelkern, J. Polymer Sci. B, 5, 557 (1967).

41. J. G. Fatou and L. Mandelkern, J. Phys. Chem. 69, 417 (1965).

42. L. Mandelkern, J. Polymer Sci. C, 15, 129 (1966).

43. L. Mandelkern, Macromolecular Preprints II, 794, IUPAC, Boston (1971).

44. L. Mandelkern, A. L. Allou, Jr., and M. R. Gopalan, J. Phys. Chem. 72, 309 (1968).

45. G. Moraglio, G. Polizzotti, F. Danusso, Eur. Polymer J. 1, 183 (1965).

46. P. Corradini, J. Polymer Sci. B, 7, 211 (1969).

47. T. Tatsumi, T. Fukushima, K. Imada, and M. Takayanagi, J. Macromol. Sci.-Phys. B1, 459 (1967).

48. C. Hendrix, D. A. Whiting, A. E. Woodward, Macromolecules 4, 548 (1970).

49. J. E. Mark, J. Amer. Chem. Soc. 88, 4354 (1966).

50. J. E. Mark, J. Amer. Chem. Soc. 89, 6829 (1967).

51. P. J. Flory, "Statistical Mechanics of Chain Molecules," Interscience, New York (1969).

52. Y. Abe and P. J. Flory, Macromolecules 4, 219 (1971).

53. R. Endo, Nippon Gomu Kyokaishi 34, 527 (1961).

54. D. J. Blundell and A. Keller, J. Macromol. Sci.-Phys. B2, 301 (1968).

55. B. Wunderlich, J. Phys. Chem. 69, 2078 (1965).

56. J. M. Stellman and A. E. Woodward, J. Polymer Sci. B7, 755 (1969).

57. J. M. Stellman and A. E. Woodward, J. Polymer Sci. A-2, 9, 54 (1971).

56. M. V. Volkenshtein, "Conformational Statistics of Polymeric Chains," Interscience, New York (1963).

57. P. J. Flory, Proc. Natl. Acad. Sci. (U.S.) 51, 1060 (1964).

58. R. A. Scott and H. A. Scheraga, J. Chem. Phys. 44, 3054 (1966).

59. R. A. Scott and H. A. Scheraga, Biopolymers 4, 237 (1966).

60. T. Ooi, R. A. Scott, E. Vanderkooi, and H. A. Scheraga, J. Chem. Phys. 46, 4410 (1967).

61. R. A. Scott and H. A. Scheraga, J. Chem. Phys. 45, 2091 (1966).

62. K. B. Wiberg, J. Amer. Chem. Soc. 87, 1070 (1965).

63. J. B. Hendrickson (a) J. Amer. Chem. Soc. 83, 4537 (1961); (b) ibid. 84, 3335 (1962); (c) ibid., 86, 4854 (1964).

64. N. L. Allinger, M. A. Miller, F. A. Van Catledge, and J. A. Hirsch, J. Amer. Chem. Soc. 89, 4345 (1967).

65. J. H. Westheimer, in "Steric Effects in Organic Chemistry," M. S. Newman, Ed., Wiley, New York (1956), Ch. 12.

66. N. A. Ahmed, A. I. Kitaigorodsky, and K_ V. Mirskaya, Acta Cryst. B27, 867 (1971).

67. A. I. Kitaigorodsky, Extra. J. Chim. Phys. 1, 9 (1966); Tetrahedron 14, 230 (1961); Acta Cryst. 18, 585 (1965).

68. G. N. Ramachandran and V. Sasisekharan, Adv. Prot. Chem. 23, 283 (1968).

69. H. Eyring, Phys. Rev. 39, 746 (1932).

70. R. St. J. Manley, J. Polymer Sci. A-2, 4503 (1964).

71. T. W. Husby and H. E. Bair, J. Appl. Phys. 39, 4969 (1968).

72. P. Corradini, V. Petraccere, and G. Allegra, Macromolecules 4, 770 (1971).

THEORETICAL AND EXPERIMENTAL INVESTIGATIONS OF THE STRUCTURE AND PROPERTIES OF POLY-(trans-1,4-BUTADIENE)

by JEANNE M. STELLMAN

Adviser: Arthur E. Woodward

ABSTRACT

The surface structure of poly-(trans-1,4-butadiene), PTBD, single crystals was quantitatively assayed by chemical reaction of the surface double bonds. The regularity of the fold surface was found to be a function of growth solvent and growth temperature. Estimates of the number of monomer units per surface fold for various solvents are given. The heats and entropies of the solid-solid transition and fusion of crystals and bulk solid were measured. The interior structure of the crystals was also found to be a function of solvent and growth temperature.

Heat capacity measurements of melt-recrystallized sample together with the entropy measurements indicated that the high-temperature form is highly defective. The presence of interior defects shows that conclusions about surface structure cannot be drawn from techniques which assay the entire crystal rather than just the surface.

Theoretical energy calculations of the solid-solid phase transition of PTBD were carried out on a computer using empirical potential energy functions. Calculations were performed on a single PTBD chain, unit cell, and lattice of cells, and the results compared. Minimization of the lattice energy with respect to the monoclinic cell constants gave results in good agreement with x-ray diffraction data, while single chain and unit cell calculations were discrepant. Large entropy effects for the defective high-temperature lattice could explain the lack of agreement of the minimization results for the high-temperature form. The energy barrier between the monoclinic and hexagonal lattices was found to be low.